Received: 16 December 2020 | Revised: 21 February 2021 | Accepted: 26 March 2021

DOI: 10.1111/bph.15475

REVIEW ARTICLE

Metabolic phenotyping of opioid and psychostimulant addiction: A novel approach for biomarker discovery and biochemical understanding of the disorder

Giorgia Caspani[1] | Viktoria Sebők[2] | Nowshin Sultana[2] | Jonathan R. Swann[1,3] | Alexis Bailey[2]

[1]Department of Metabolism, Digestion and Reproduction, Faculty of Medicine, Imperial College London, London, UK

[2]Pharmacology Section, Institute of Medical and Biomedical Education, St George's, University of London, London, UK

[3]School of Human Development and Health, Faculty of Medicine, University of Southampton, Southampton, UK

Correspondence
Alexis Bailey, Pharmacology Section, Institute of Medical and Biomedical Education, St George's, University of London, London, UK.
Email: abailey@sgul.ac.uk

Jonathan R. Swann, Department of Metabolism, Digestion and Reproduction, Faculty of Medicine, Imperial College London, London, UK.
Email: j.swann@imperial.ac.uk

Funding information
Medical Research Council, Grant/Award Number: MR/N014103/1

Despite the progress in characterising the pharmacological profile of drugs of abuse, their precise biochemical impact remains unclear. The metabolome reflects the multi-faceted biochemical processes occurring within a biological system. This includes those encoded in the genome but also those arising from environmental/exogenous exposures and interactions between the two. Using metabolomics, the biochemical derangements associated with substance abuse can be determined as the individual transitions from recreational drug to chronic use (dependence). By understanding the biomolecular perturbations along this time course and how they vary across individuals, metabolomics can elucidate biochemical mechanisms of the addiction cycle (dependence/withdrawal/relapse) and predict prognosis (recovery/relapse). In this review, we summarise human and animal metabolomic studies in the field of opioid and psychostimulant addiction. We highlight the importance of metabolomics as a powerful approach for biomarker discovery and its potential to guide personalised pharmacotherapeutic strategies for addiction targeted towards the individual's metabolome.

KEYWORDS
addiction, cocaine, heroin, metabolism, metabolomics, methamphetamine, morphine

1 | METABOLOMICS AS A TOOL TO UNDERSTAND DRUG ADDICTION

Drug addiction is a chronic relapsing brain disorder characterised by compulsive drug seeking, loss of control over drug intake and the emergence of physical and emotional withdrawal symptoms when the drug is absent (Koob & Kreek, 2007; Koob & Le Moal, 2001; Wee & Koob, 2010). It is thought to arise, at least partly, as a result of the long-term compensatory mechanisms that occur in response to the increase in striatal dopaminergic transmission along the mesolimbic pathway elicited by drug use. However, a detailed and refined understanding of the biochemical processes underlying addiction and the nature of the profound interpersonal variability in drug responses and progression of the disorder is still unclear.

Abbreviations: 5-HIAA, 5-hydroxyindoleacetic acid; DOPAC, 3,4-dihydroxyphenylacetic acid; Gln–Glu–GABA, glutamine–glutamate–GABA; SIRT1, Sirtuin 1; TCA, tricarboxylic acid; Trx-1, thioredoxin-1.

Giorgia Caspani and Viktoria Sebők; Jonathan R. Swann and Alexis Bailey contributed equally to this study.

The observation that addicted individuals present a range of metabolic abnormalities led to the notion of drug addiction as a 'metabolic disease' (Dole & Nyswander, 1967). Thus, a global investigation of the biochemical perturbations characteristic of the disease may be successful in providing mechanistic insights into disease states and progression. Metabolomics uses high-resolution analytical chemistry techniques to simultaneously measure a large number of low MW molecules in a biological sample. This results in large datasets where the variables (i.e. metabolites) largely outnumber the observations (i.e. mice or human participants). As such, appropriate dimensionality reduction techniques are necessary to analyse the entire metabolic profile in relation to an outcome of interest (Worley & Powers, 2013). Multivariate models can be constructed to predict class membership (e.g.,disease state) or a continuous response variable (e.g. behavioural data) from linear combinations of the original variables (Saccenti et al., 2014). The predictive ability and significance of the model can then be assessed through cross-validation and permutation testing, respectively. While acknowledging the interrelation of metabolites, multivariate methods allow for assessing the 'weight' or contribution of each metabolite to the overall predictive model (Saccenti et al., 2014), aiding the identification of potential biomarkers. This unique biochemical fingerprint, referred to as the metabolome, reflects the metabolic processes occurring in the biological system at the time of analysis and its overall metabolic status (Kosmides et al., 2013). In addition, the metabolome contains exogenous molecules entering the system (e.g. dietary factors and xenobiotics) and products resulting from their breakdown. Drug addiction is a unique disorder in that it arises from the combination of genetic risk factors and exposure to an exogenous substance (i.e. drug of abuse). By capturing the 'metabolic phenotype' originating from both endogenous processes and the interaction with exogenous molecules (Figure 1), metabolomics provides a unique technique to investigate the biochemical basis of addiction.

Metabolomic approaches are also a powerful tool for biomarker discovery. As the fourth most costly mental disorder in the European Union (Gustavsson et al., 2011), addiction is a major public health issue with serious socio-economic implications and efforts continue to be made to improve the diagnosis and management of this disorder. The diagnosis of drug addiction is based solely on identifying characteristic symptoms and behaviours in accordance with the Diagnostic and Statistical Manual of Mental Disorders Fifth Edition (American Psychiatric Association, 2000). No reliable diagnostic test currently exists for primordially predicting drug addiction vulnerability and for identifying individuals at risk of relapse or at risk of co-morbidity. When pharmacological options for managing addiction symptomology are available (e.g. **methadone**/**buprenorphine** for opioid withdrawal and **naloxone** for craving), efficacy is often limited and responses are highly variable. It also remains impossible to predict the efficacy and potential side effects of pharmacotherapy on an individual basis. These challenges demonstrate the need for quantitative biomarkers to predict an individual's addiction risk, disease progression, relapse vulnerability and response to interventional strategies. Pharmacometabolomics is a branch of metabolomics whereby an individual's baseline metabolic phenotype is used to predict their handling and response to a pharmacological intervention (Kaddurah-Daouk & Weinshilboum, 2014). As our understanding in

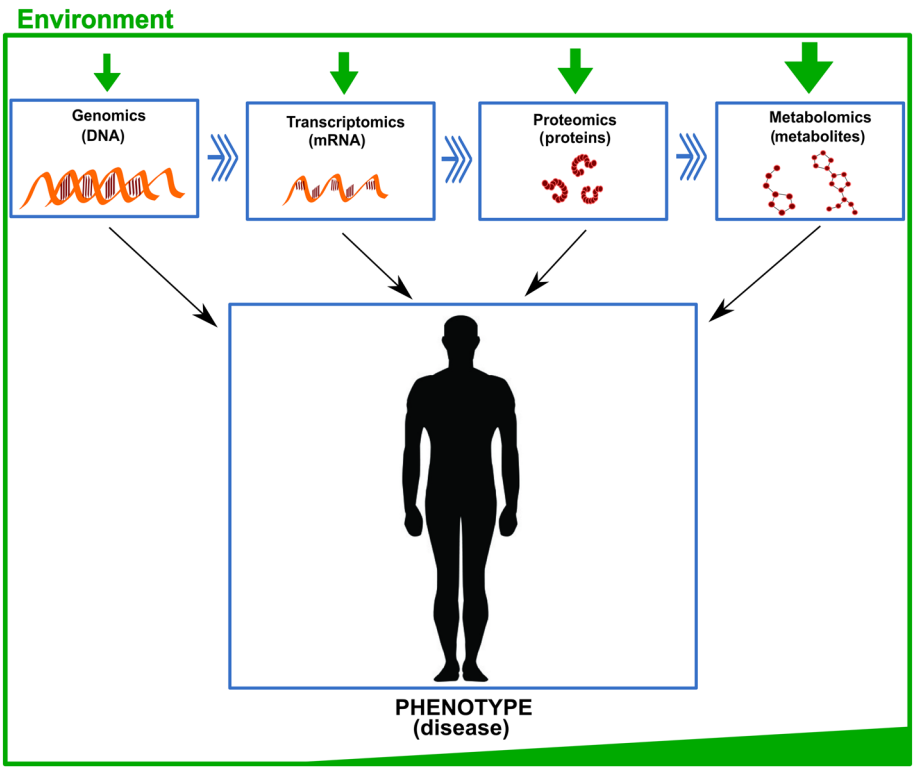

FIGURE 1 Each level of the 'omics' cascade gives a different level of insight into the phenotype. The interaction of each component (genome, transcriptome, proteome and metabolome) with the environment (nutrition, stress and drugs) influences the resulting phenotype and can contribute to disease. The size of the green arrows indicates the influence of the environment increases on each level of the omics cascade and is highly reflected by the metabolome. Although each omics technique can reveal important diagnostic and prognostic biomarkers of disease, the ability of metabolomics to capture both endogenous (i.e. genetic) and exogenous (i.e. environmental and drug-related) influences on the observed disease phenotype, its chemical diversity and dynamic nature, suggests that metabolic biomarkers may better represent the resulting phenotype of drug abuse

this area grows, a personalised approach to care delivery and clinical decision making in the management of substance abuse disorders may become possible.

This review summarises the findings of published studies in humans and rodent models investigating the biomolecular perturbations elicited by opioids and psychostimulants on the brain (target organ) and peripheral tissues/biofluids with translational value (e.g., blood, urine and hair). As our understanding in this area grows, a personalised approach to care delivery and clinical decision making in the management of substance abuse disorders may become possible.

2 | METABOLIC PHENOTYPING OF OPIOID ADDICTION

Opioids, such as **morphine** and **heroin**, are highly addictive substances. Their rewarding effects are mediated by their ability to induce **dopamine** transmission in the nucleus accumbens by relieving the inhibition of **GABA**ergic interneurons on mesolimbic dopamine-releasing neurons in the ventral tegmental area (Spanagel & Weiss, 1999). The following section provides an overview of animal and human studies investigating the metabolic changes associated with the distinct stages of opioid (morphine and heroin) addiction. Although the analysis of brain samples can help unravel biochemical pathways affected by repeated opioid administration (Deng et al., 2012; Gao et al., 2007; Hu et al., 2012; Li et al., 2017) or involved in the reinforcing effects of the drugs (Meng et al., 2012), sequential sampling of plasma and urine samples allows for the identification of biomarkers of the different addiction states (i.e. euphoria, tolerance, abstinence and withdrawal, Liu et al., 2015; Zaitsu et al., 2014) and predictors of treatment outcome (i.e. response and relapse, Ning et al., 2018; Zheng et al., 2013). Human studies have also been conducted to understand the perturbations in the hair metabolome driven by heroin (Xie et al., 2016) and to investigate the metabolic changes induced by withdrawal from opioids (Mannelli et al., 2009). These studies are summarised in Table 1.

2.1 | Metabolic signature of morphine addiction

^{1}H-NMR spectroscopy-based studies of the metabolic abnormalities induced by repeated morphine administration on brain samples were conducted in rhesus monkeys (Deng et al., 2012) and rodents (Gao et al., 2007; Hu et al., 2012). Significant disturbances in the **glutamine**–**glutamate**–GABA (Gln–Glu–GABA) axis, which are markers of oxidative stress and involved in neurotransmission, were a common finding. The specific changes reported varied depending on the species and the brain region considered and are reviewed in Table 2. Some discrepancies regarding the direction of change of these metabolites may also be underpinned by differences in experimental design (e.g. dose and length of drug administration; see Table 1). Disturbances in the equilibrium state between GABA, Glu and Gln, with a general increase of GABA and decrease in Glu, were consistent with microdialysis studies showing increased GABA and decreased Glu within the medial prefrontal cortex (Ramshini et al., 2019), nucleus accumbens (Sun, Yang, et al., 2011) and hippocampus (Kang et al., 2006) in response to morphine. Such changes were ascribed to alterations in tricarboxylic acid (TCA) cycle activity and enhanced conversion of Glu into GABA by GAD. A decrease in GABA degradation has also been suggested (Gao et al., 2007). The shift in the Gln–Glu–GABA equilibrium state observed in these studies may also be the result of neuroadaptations caused by the effect of morphine on GABAergic neurotransmission, which is known to mediate the rewarding properties of opioids. This is supported by evidence suggesting that GABA and activation of the GABAergic system attenuates the reinforcing effects of drugs of abuse via its modulatory effect on the mesolimbic dopaminergic pathway (Tsuji et al., 1996; Westerink et al., 1996) and that its disruption is involved in the development of tolerance and dependence to opioids (Hu et al., 2012; Sepúlveda et al., 2004). These metabolic changes were not evident until Day 10 of morphine administration, suggesting that long-term adaptive mechanisms underlie these alterations (Gao et al., 2007). The membrane constituent phosphocholine and the phosphoinositol precursor **myo-inositol** were dysregulated in response to morphine exposure, indicating an effect of morphine on membrane integrity. *Myo*-inositol is also an osmolyte highly expressed in glial cells. Changes in the abundance of *myo*-inositol and the neuronal marker *N*-acetylaspartate (NAA) may reflect glial hypertrophy and altered neuronal morphology and activity. Glial cells are emerging as an important player in addiction pathophysiology due to their role in supporting neurotransmission and brain energy metabolism (Miguel-Hidalgo, 2009). Morphine has been shown to affect neuronal maturation *in vitro* by modulating astrocytic proliferation (Stiene-Martin et al., 1991). Irrespective of species and brain regions considered, an increase in **lactic acid** was observed in all studies (Deng et al., 2012; Hu et al., 2012). Lactic acid is the end product of anaerobic cellular metabolism and is produced when energy demand exceeds the rate of oxidative metabolism. Elevated lactic acid indicates tissue damage and impaired **pyruvate** oxidation (Veech, 1991). Given that lactate can only be completely oxidised in mitochondria, increased lactic acid observed in these studies is likely to be an indication of mitochondrial dysfunction, energy metabolism impairment, oxidative stress and/or up-regulation of the enzyme LDH. Consistently, metabolites related to oxidative stress such as the antioxidants **glutathione**, **taurine** and **creatine** also showed a large deviation from controls following repeated morphine administration. Feng et al. (2013) suggested hippocampal mitochondrial damage and decreased mitochondrial DNA copy number as a hallmark of addiction. Using cultured rat **pheochromocytoma** cells and mouse neurons treated with morphine, the authors showed that oxidative stress caused by morphine administration led to mitochondrial damage and autophagy. Given the involvement of mitochondria in synaptic remodelling, mitochondrial dysfunction is likely to have downstream effects on synaptic plasticity and neurotransmission, with an inevitable downstream impact on the addiction cycle (Figure 2). In support of this hypothesis, the up-regulation of ROS in the hippocampus, as a result of morphine

TABLE 1 Summary of animal and human studies

Drug	Protocol	Species/participants	Tissue(s)/fluid(s)
Morphine	90-day escalating dose of drug 3–15 mg·kg^{-1} three times per day (s.c.) followed by 7-day detoxification period (6-mg·kg^{-1} methadone or 0.02-mg·kg^{-1} clonidine [i.g.] three times per day)	Rhesus monkeys	Hi and PFC
	14-day escalating dose of drug 5–40 mg·kg^{-1} two times per day (i.p.) followed by detoxification with 10-mg·kg^{-1} methadone or 0.2-mg·kg^{-1} clonidine (i.g.) (three administrations at 12-h intervals)	Male Sprague–Dawley rats	Hi, PFC, NAc and Str
	10 mg·kg^{-1} two times per day of drug for 1, 6 or 10 days (i.p.)	Male Sprague–Dawley rats	Hi and PFC
	10-day administration group underwent 1, 3 or 5 days of abstinence		
	Alternating morphine (4 mg·kg^{-1} [s.c.]) or saline (10 ml·kg^{-1} [s.c.]) + 7-day CPP	Male ICR mice	Whole brain
	4 mg·kg^{-1} + 10-day CPP	Male Sprague–Dawley rats	Plasma and urine
	5-day escalating dose of drug 10–50 mg·kg^{-1} three times per day (i.p.) followed by 5-mg·kg^{-1} naloxone (i.p.)	Male Sprague–Dawley rats	Plasma
	6-day inpatient detoxification with methadone (30 mg on Day 1, tapered by 5 mg daily)	14 opioid-dependent individuals enrolled in methadone detoxification programme and 10 nondependent controls	Plasma

TABLE 1 (Continued)

Drug	Protocol	Species/participants	Tissue(s)/fluid(s)
Heroin	10-day escalating dose of drug 3–16.5 mg·kg^{-1} two times per day (i.p.) followed by 4 days of abstinence, followed by 4 days of relapse period (16.5-mg·kg^{-1} heroin, i.p., once a day for 4 days)	Male Sprague–Dawley rats	Serum and urine
	Chronic administration (15 mmol·kg^{-1}, i.p., twice a day) for 12 days; withdrawal group given saline for the last 2 days	Male C57BL/6J mice	Brain
	Self-administration: infusion (0.06 mg·kg^{-1}); followed by 14 days of abstinence	Male Sprague–Dawley rats	Serum
	Hair collected from vertex posterior region of the head Consumption of heroin was confirmed by blood testing	58 heroin abusers and 72 nonheroin abusers	Hair
	Acute 30-mg·kg^{-1} administration (i.p.)	Male Sprague–Dawley rats	Frontal cortex, left and right Str, and Th
	Single administration: 20 mg·kg^{-1} (i.p.), killed after 2, 24 or 48 h		
	Repeated administration: 10 or 20 mg·kg^{-1} (i.p.), 7-day CPP conditioning	Male Wistar rats	NAc and Str
	Repeated administration: 20 mg·kg^{-1} (i.p.), 7 days but with no CPP		
	Repeated administration: 20 mg·kg^{-1} (i.p.), 6-day CPP conditioning 20 mg·kg^{-1}	C57BL/6J mice (6–8 weeks old)	VTA and NAc
	20 mg·kg^{-1} (i.p.)	Male Wistar rats	Brain (PFC, Cer, Hi or Str) and plasma

(Continues)

TABLE 1 (Continued)

Drug	Protocol	Species/participants	Tissue(s)/fluid(s)
	7-day pretreatment with nicotine (50 μg·ml) followed by cocaine + 4-day CPP	Male C57BL/6J mice	Brain (NAc and Str)
		(B) 2-mg·kg^{-1} cocaine	
	(C) 20-mg·kg^{-1} cocaine		
	(D) Nicotine	Altered neurotransmission, energy homeostasis and cell metabolism	
	(E) Nicotine + 2-mg·kg^{-1} cocaine		
	Self-administration for 6 h·day^{-1} or up to 50 infusions per day, followed by extinction (cocaine replaced with saline) for 8 days and reinstatement (10 mg·kg^{-1}, i.p.)	Rats (species unspecified)	Serum
	10 mg·kg^{-1} (i.p.) + 10-day CPP	Male Sprague–Dawley rats	Plasma and urine
	1-day or 3-week withdrawal after self-administration training	Male Sprague–Dawley rats	Brain (Str, PFC and NAc)
	21 days of 105-min daily infusions of (i) cocaine (15 mg·kg^{-1}); (ii) alcohol (2 g·kg^{-1}); (iii) cocaine + alcohol (15 mg·kg^{-1} and 2 g·kg^{-1}, respectively); and (iv) 0.9% (w/v) sodium chloride solution (control group)	Male and female Wistar rats	Plasma
	Blood collected in the morning after 8-h fasting	44 crack-cocaine users and 44 healthy volunteers (males only)	Serum
	>2 weeks of abstinence (monitored by urine drug screens three times a week for 2 weeks)	18 cocaine-dependent individuals and 10 healthy controls	Plasma
Methamphetamine	10-mg·kg^{-1} administration every hour (four injections) (i.p.)	Male Sprague–Dawley rats	Plasma and urine
	Sample collection:		
	Group A: 0–24 h (urine) or 24 h (plasma) after treatment		
	Group B: 72–96 h (urine) or 96 h (plasma) after treatment		

TABLE 1 (Continued)

Drug	Protocol	Species/participants	Tissue(s)/fluid(s)
	Single exposure:10 mg·kg^{-1} followed by 10- to 30-mg·kg^{-1}·day^{-1} escalating dose for 5 days followed by 2 days of drug-free detoxification	Male Sprague–Dawley rats	Serum and urine
	Plasma collected immediately after 16 days of MA self-administration (SA) and after 12 and 24 h of abstinence	Male Sprague–Dawley rats	Plasma
	2 mg·kg^{-1}, i.p. + 10-day CPP	Male Sprague–Dawley rats	Plasma and urine
	2.5-mg·kg^{-1} drug twice a day for 7 days (s.c.)	Male Wistar rats	Hi, NAc and PFC
	Locomotor measurements on Days 0, 1, 3 and 5 following injections (sensitisation)		
	Single 3-mg·kg^{-1} dose or five daily injections (i.p.)	Eight different strains of male mice: 129S1/SvImJ, A/J, C3H/HeJ, C57BL/6J, CAST/EiJ, DBA/2J, NOD/ShiLtJ and PWD/PhJ	Whole brain
	3-mg·kg^{-1} drug once a day for 5 days (i.p.)	Eight different strains of male mice: 129S1/SvImJ, A/J, C3H/HeJ, C57BL/6J, CAST/EiJ, DBA/2J, NOD/ShiLtJ and PWD/PhJ	Whole brain
	1 mg·kg^{-1} (i.p.) + 6-day CPP	Male Sprague–Dawley rats	Brain (NAc and dorsal and ventral Hi)
	Control diet or diet supplemented with 0.6% (w/v) METH	Virgin male *Drosophila melanogaster*	Whole organism
	Daily 2-h self-administration sessions (i.v., 0.05 mg·kg^{-1} per injection)	Male Sprague–Dawley rats	Urine and hair
	Sample collection at baseline (M1 = 'drug-free'), after stable lever press responding to methamphetamine (M2 = 'reward') and after methamphetamine following extinction with saline (M3 = 'relapse')		
	3-cm hair strands from the root	10 heavy MA abusers and 12 drug-free controls	Hair
	Blood collected in the morning at fasting	30 METH abusers and 30 healthy controls (males only)	Serum

Abbreviations: 5-HIAA, 5-hydroxyindoleacetic acid; Cer, cerebellum; CPP, conditioned-place preference; DOPAC, 3,4-dihydroxyphenylacetic acid; GC-MC, gas chromatography-mass spectrometry; GPC, glycerol phosphocholine; GSH/GSSG, GSH/oxidised GSH; 3-HB, 3-hydroxybutyric acid; Hi, hippocampus; LC, liquid chromatography,NAA, *N*-acetylaspartate; NAc, nucleus accumbens; NAG, *N*-acetyl-glycoprotein; OAG, *O*-acetyl-glycoprotein; Pc, phosphocholine; PFC, prefrontal cortex; Str, striatum; TCA, tricarboxylic acid; Th, thalamus; VTA, ventral tegmental area.

TABLE 1 (Continued)

Drug	Main results	Altered metabolites (drug of abuse vs. control)	Analytical method	Reference
Morphine	Shift in the equilibrium of Gln–Glu–GABA axis	Hi: ↑ glutamine, GABA and lactic acid	^{1}H-NMR spectroscopy (600 MHz)	Deng et al., 2012
	Significant membrane and energy metabolism disruption	↓ glutamate, GABA, succinic acid semialdehyde, GSH, NAA, Pc, *myo*-inositol, taurine, lactic acid and creatine		
	Methadone/clonidine treatment reversed most metabolites except glutamate	PFC: ↑ succinic acid semialdehyde, NAA, Pc, lactic acid and creatine		
	See Tables 2 and 3 for details	↓ glutamate, GABA, *myo*-inositol and taurine		
	Shift in the equilibrium of Gln–Glu–GABA axis	Hi: ↑ glutamate, succinic acid semialdehyde, NAA, lactic acid and creatine; ↓ glutamine, GABA, Pc and *myo*-inositol	^{1}H-NMR spectroscopy (600 MHz)	Hu et al., 2012
	Significant membrane and energy metabolism disruption	PFC: ↑ GABA, succinic acid semialdehyde and lactic acid; ↓ glutamine, glutamate, GSH, *myo*-inositol and creatine		
	Methadone and clonidine reversed most metabolites, but clonidine restored metabolites, which methadone was ineffective for	NAc: ↑ glutamine, glutamate, GABA, succinic acid semialdehyde, GSH, NAA, taurine, lactic acid and creatine; ↓ *myo*-inositol		
	See Table 2 for details	Str: ↑ glutamine, glutamate, GABA, succinic acid semialdehyde, GSH, NAA, Pc, taurine and lactic acid; ↓ *myo*-inositol and creatine		
	Significant disturbance of Gln–Glu–GABA axis and other metabolites after 10 days of administration (see Table 2)	Hi: ↑ glutamine and *myo*-inositol; ↓ glutamate, GABA, NAA and taurine	^{1}H-NMR spectroscopy (800 MHz)	Gao et al., 2007
	Even 3-day-long withdrawal period normalises metabolites	PFC: ↑ GABA and *myo*-inositol; ↓ glutamate		
	21 significantly altered metabolites between morphine and control groups	↑ carbodiimide, 2-methyl-propanoic acid, aminoethyl alcohol, L-proline, 3-hydroxybutanoic acid, L-valine, ethanedioic acid, uracil, D-mannofuranoside, 4(3*H*)-quinazolinone, 2-methyl-3-[2-methyl-3-[(trimethylsilyl) oxy]phenyl]-, niacinamide, 2,3-dimethyl-3-hydroxyglutaric acid, pyrogallol, dodecanoic acid, 2-hexenedioic acid, 2-hydoxy-1,2,3-propanetricarboxylic acid,	GC–MS	Meng et al., 2012
	Myo-inositol, *myo*-inositol phosphate, nicotinamide, proline and valine reflect abnormal intracellular signal transduction pathway in morphine-induced CPP			

TABLE 1 (Continued)

Drug	Main results	Altered metabolites (drug of abuse vs. control)	Analytical method	Reference
		myo-inositol, D-glucopyranose phosphate and *myo*-inositol phosphate		
	PCA and ROC analysis revealed clear separation with an AUC value of 0.947	↓ arabinonic acid and cholesterol		
	Full separation of urine samples on TCA due to 12 metabolites	Plasma: ↑ *N*-propylamine; ↓ 3-hydroxybutyric acid, L-tryptophan and cystine	GC–MS	Zaitsu et al., 2014
	Partial separation in plasma samples due to four metabolites PLS regression model based on these could predict CPP scores	Urine: ↑ 2-ketoglutaric acid, fumaric acid, malic acid and L-threonine; ↓ glutamic acid, isoleucine, L-valine, L-aspartic acid, oxamic acid, 2-aminoethanol, indoxyl sulfate and creatinine		
	11 organic acids, 13 amino acids, 6 sugars and 6 fatty acids discriminated between groups	Morphine vs. control groups: ↑ oxalic acid, aminomalonate, β-D-glucose, linoleic acid, stearic acid and cholesterol; ↓ alanine, proline, glycine, serine, threonine, pyroglutamic acid, hydroxyproline, erythronic acid, glutamine, arabinose and rhamnose	GC–MS	Liu et al., 2015
	PLS-DA model could discriminate between euphoria, withdrawal and tolerance groups	Naloxone vs. control groups: ↑ lactic acid, oxalic acid, aminomalonate, oxoglutaric acid, β-D-glucose, linoleic acid, cholesterol and palmitic acid; ↓ alanine, valine, proline, glycine, serine, threonine, pyroglutamic acid, hydroxyproline, erythronic acid, glutamine, arabinose, rhamnose, isoleucine, succinate, 4-hydroxybutanoic acid and leucine		
	Overactivity of oxidation–reduction pathways, and purine and monoamice metabolism	↑ GSH/GSSG, α-tocopherol and γ-tocopherol ↑ guanine and xanthosine; ↓ guanosine, hypoxanthine, hypoxanthine/xanthine and xanthine/xanthosine ↑ *N*-methyl-5-HT	LC electrochemical array detection (LCECA)	Mannelli et al., 2009
Heroin	Urine and serum metabolites show similar trend of changes throughout the study	Serum: ↑ aspartate, leucine, valine, phenylalanine, threonine, citrate, *myo*-inositol-1-phosphate, *myo*-inositol and thiamine; ↓ hydroxyproline, tryptophan, 5-HT, threonate, creatine and nonesterified cholesterol	GC–MS	Zheng et al., 2013

(Continues)

TABLE 1 (Continued)

Drug	Main results	Altered metabolites (drug of abuse vs. control)	Analytical method	Reference
	Metabolome of withdrawn rats tend back to baseline, except *myo*-inositol, citrate and threonate	Urine: ↑ pyroglutamate, spermidine, tryptophan, citrate, aconitate, *myo*-inositol and glucuronate; ↓ aspartate, glycine, β-alanine, hyrdoxyproline, fumarate, lactate and octadecanoic acid		
	Metabolic state of relapse is closer to 10-day exposure group			
	Altered amino acids, TCA cycle intermediates, neurotransmitters, nucleotides and other compounds	Withdrawal: ↓ histidine and melatonin; ↑ phenylalanine and tryptophan, *N*-acetyl-5-HT and restored catecholamines	UPLC-TOF/MS	Li et al., 2017
	Impaired energy production, altered fatty acid metabolism and altered neurotransmission	↑ choline, PC, GPC, glucose, 3-HB, acetoacetate, glutamine, phenylalanine, acetate, NAG and OAG	^{1}H-NMR spectroscopy (600 MHz)	Ning et al., 2018
		↓ fumarate, pyruvate, histamine, lactate and lipid		
	Possible up-regulation of the HPA axis	↑ sorbitol and cortisol	UFLC-ITTOF	Xie et al., 2016
		↓ myristic acid, linoleic acid, arachidonic acid, GSH and three unknown compounds		
	Global metabolic analysis showed separation of control vs. cocaine-treated brains	PFC: ↑ 5-HT, norepinephrine, glucose, dopamine and DOPAC; ↓ 5-HIAA	IMMS for global metabolites	Kaplan et al., 2013
	Standard addition to characterise biogenic amine level response to acute cocaine	Str: ↑ norepinephrine; ↓ glucose, dopamine and DOPAC	Isotope dilution for (glucose)	
		Th: ↑ 5-HT, dopamine, DOPAC and 5-HIAA; ↓ norepinephrine and glucose	Standard addition for NE, 5-HT, 5-HIAA, DA and DOPAC	
	Even single exposure causes oxidative stress (OS) and lasting changes in metabolites	Repeated administration (CPP): NAc: ↑ lactate, NAA, acetylcysteine, glutamate, succinate, GABA, creatine and taurine; ↓ leucine, 3-hydroxybutyric acid, L-lysine, cysteine and *myo*-inositol	^{1}H-NMR spectroscopy (600 MHz)	Li et al., 2012
		Repeated administration (no CPP): NAc: ↑ NAA, succinate, creatine and taurine		
	Repeated treatment caused mitochondrial dysfunction and membrane disruption, neurotransmitter deviation and OS	Repeated administration (CPP): Str: ↑ NAA, GABA, taurine and choline; ↓ 3-HB, lactate, creatine, glycerol and *myo*-inositol		

TABLE 1 (Continued)

Drug	Main results	Altered metabolites (drug of abuse vs. control)	Analytical method	Reference
		Repeated administration (no CPP): Str: ↑ GABA		
	Rats treated with CPP and without CPP separated based on their metabolites with PLS-OSC	Single exposure—2 h: ↑ NAA, *myo*-inositol and cysteine; ↓ lactate, creatine, choline, taurine, glycine and Pc		
		Single exposure—24 h: ↑ NAA, *myo*-inositol, creatine, taurine and cysteine; ↓ lactate, choline, glycine and Pc		
	Separation also between 2-, 24- and 48-h groups	Single exposure—48 h: ↑ NAA, choline, taurine and glycine; ↓ lactate, *myo*-inositol, cysteine and Pc		
	Altered energy metabolism and epigenetic regulation	↑ nicotinamide mononucleotide (NMN) and nicotinamide adenine dinucleotide (NAD), blocked by specific nicotinamide phosphoribosyltransferase (NAMPT) inhibitor FK866	^{1}H-NMR spectroscopy (600 MHz)	Kong et al., 2018
	Altered neurotransmission	PFC: ↑ ACh	LC–MS/MS	Olesti et al., 2019
		Cer: ↑ glutamate, choline, ACh, carnitine and creatinine		
		Hi: ↑ valine, leucine, GABA, glutamate, choline, ACh, carnitine, acetylcarnitine, creatine, creatinine and adenosine		
		Str: ↑ choline and adenosine		
		Plasma: ↑ choline and creatine; ↓ creatinine		
		20-mg·kg^{-1} cocaine vs. control:	^{1}H-NMR spectroscopy (600 MHz)	Li et al., 2014
		NAc: ↑ glutamate, tryptamine, glucose, 1-methylhistidine and proline		
	Nicotine enhances cocaine-induced CPP (2-mg·kg^{-1} cocaine with nicotine	NAc: ↓ lactate, ACh, L-glutamine, L-methionine, creatine, α-ketoglutaric acid and Pc		

(Continues)

TABLE 1 (Continued)

Drug	Main results	Altered metabolites (drug of abuse vs. control)	Analytical method	Reference
	pretreatment was similar to 20-mg·kg^{-1} cocaine only)			
		Str: ↑ glutamate, 1-methylhistidine and glucose		
		Str: ↓ lactate, α-ketoglutaric acid and L-glutamine		
	Similar metabolic effects of nicotine pretreatment and low cocaine dose and high cocaine only	Nicotine + 2-mg·kg^{-1} cocaine vs. control		
		NAc: ↑ glutamate, 1-methylhistidine and proline		
		NAc: ↓ tryptamine, lactate, L-glutamine, L-methionine, creatine and α-ketoglutaric acid		
	Altered neurotransmission, energy homeostasis and cell metabolism	Str: ↑ glutamate		
		Str: ↓ α-ketoglutaric acid and L-glutamine		
	Only a subset of features was investigated, due to the primary aim of the study to evaluate the application of the MEDI method to discriminate phenotypic groups based on mass spectroscopy signals	↑ 3-methylene-indolenine (3-methoxy-4-hydroxyphenyl)ethylene glycol, kynurenic acid, deoxyuridine, thymidine estradiol, GSH, 3-indole carboxylic acid glucuronide, 5-hydroxy-6-methoxyindole, glucuronide, dityrosine, LPE (20:5) and LPC (18:2)	UPLC-IM-MS and UPLC-IM-MSE	Goodwin et al., 2014
	This method (based on self-organising maps) allows for the discrimination of cocaine-addicted, cocaine-nonaddicted and cocaine-naïve rats			
	No separation of urine and partial separation of plasma	Plasma: ↑ threonine and *n*-propylamine; ↓ cystine and spermidine; no differences detected in urine	GC–MS	Zaitsu et al., 2014
	Altered markers of OS, energy metabolism and membrane integrity	Str (1 day): ↑ creatinine, pyroglutamic acid and adenosine; ↓ choline	HPLC-IMMS	Zhang, Xue, et al., 2016
		Str (3 weeks): ↑ creatinine, spermidine, carnosine and adenosine		

TABLE 1 (Continued)

Drug	Main results	Altered metabolites (drug of abuse vs. control)	Analytical method	Reference
		PFC (1 day): ↑ GABA, creatinine and adenosine; ↓ creatine and glutamate		
		NAc (1 day): ↑ glutamate; ↓ niacinamide, glutamine and adenosine		
	Altered amino acid metabolism	Cocaine vs. control: ↑ methionine; ↓ argininosuccinic acid and *N*-ε-acetyl-L-lysine	LC–MS	Sánchez-López et al., 2017
		Cocaine + alcohol vs. control: ↑ carnosine, spermidine and 5-HT; ↓ methionine, argininosuccinic acid and *N*-ε-acetyl-L-lysine		
	Altered histamine and dopamine metabolism?	↑ lactate, histidine and tyrosine	NMR	Costa et al., 2019
		↓ long-chain fatty acid, carnitine and acylcarnitines		
	N-Methyl-5-HT and xanthine can predict addiction severity	↑ *N*-methyl-5-HT and guanine	LCECA	Patkar et al., 2009
	N-Methyl-5-HT, xanthine, xanthosine, and guanine differentiated cocaine and control groups	↓ hypoxanthine, anthranilate and xanthine		
Methamphetamine		Group A:	GC–MS and CE-MS	Shima et al., 2011
	Both urine and plasma of treated animals separated from controls on PCA scores after 24 h, but all metabolites restored after 96 h	Plasma: ↑ glucose; ↓ 3-HB		
	Decreased TCA intermediates in both urine and plasma indicate energy production inhibition	Urine: ↑ 5-oxoproline, saccharic acid and uracil; ↓ TCA cycle intermediates (including aconitate, α-ketoglutarate, malate, fumarate, succinate, oxaloacetate/pyruvate and isocitrate/citrate), 3-HB and adipic acid		
		Group B: metabolic disturbances observed in Group A returned to baseline levels		
	Disruption of amino acid, inositol and lipid metabolism and TCA cycle (energy interruption and increased physical activity)	Serum: ↑ asparatate, glutamate, glutamine, tryptophan, lysine, *cis*-9-hexadecenoic acid, 3-HB, fumarate and galactonolacetone; ↓ alanine, glycine, proline, serine, threonine, valine, leucine, isoleucine, taurine, monopalmitin, oleic acid, palmitic acid, heptadecanic acid, stearic acid, glycerol, glycerol-3-phosphate, α-aminoisobutyrate,	GC–MS	Zheng et al., 2014

(Continues)

TABLE 1 (Continued)

Drug	Main results	Altered metabolites (drug of abuse vs. control)	Analytical method	Reference
		aminomalonic acid, α-ketoglutarate, citrate, pyruvate, succinate, glucose, creatine, indoleacetate, *myo*-inositol and lactate		
		Urine: ↑ alanine, glutamate, glycine, serine, palmitic acid, 3-HB, glycerol, citrate, pyruvate, fumarate, succinate, *myo*-inositol and lactate; ↓ heptadecanic acid, stearic acid and hippurate		
	Greatest separation observed between 24-h abstinence and control mice (untargeted) and between 24-h abstinence and self-administering rats (targeted)	SA vs. control: ↑ hexadecanoylcarnitine, octadecanoylcarnitine, octadecadienylcarnitine and acetylcarnitine; 5-HT; PC (aa 30:0 and 32:0; ae 34:0 and 34:1); and SM 18:0	UPLC-QTOF-ESI-MS (untargeted) and (LC)-QQQ-MS (targeted)	Kim et al., 2020
	Variance explained largely by amino acid metabolism	↓ carnitine; alanine, arginine, asparagine, citrulline, glutamine, glycine, histidine, isoleucine, leucine, lysine, methionine, ornithinine, phenylalanine, proline, serine, threonine, tryptophan, tyrosine, valine, acetylornithine, asymmetric dimethylarginine, carnosine, creatinine, methionine sulfoxide, putrescine, spermidine, *trans*-4-hydroxyproline and dimethylarginine		
	Disrupted metabolic pathways involved in energy metabolism, the nervous system and membrane lipid metabolism	↓ lyso PC (16:0, 16:1, 17:0, 18:0, 18:1, 18:2, 20:3, 20:4, 26:0 and 26:1); PC (aa 36:0, 36:2, 36:3, 36:4, 38:0, 38:5, 38:6, 40:4, 40:5, 40:6, 42:5 and 42:6; ae 38:2, 38:4, 40:4, 40:5, 40:6, 42:1, 42:2, 42:3 and 44:6); and SM (OH) 22:2		
	No significant separation observed between treated and control animals, neither in plasma nor in urine	Plasma: ↑ *N*-propylamine; ↓ lauric acid	GC–MS	Zaitsu et al., 2014
	Few metabolite changes are not enough to have caused a PCA score separation, and their biological significance is unclear	Urine: ↑ lactose, spermidine and stearic acid		
	Unchanged energy metabolites			
		Hi: ↑ homocysteic acid, *myo*-inositol, succinic acid semualdehyde and ADP; ↓ GABA, glutamate, glutamine, NAA, GSH,	^{1}H-NMR spectroscopy (600 MHz)	Bu et al., 2013

TABLE 1 (Continued)

Drug	Main results	Altered metabolites (drug of abuse vs. control)	Analytical method	Reference
		acetylcysteine, methionine, α-ketoglutarate, succinate and citrate		
	Metabolite shifts indicate disruption of GABAergic function and membranes, OS and mitochondrial dysfunction	NAc: ↑ Pc and homocysteic acid; ↓ GABA, glutamate, glutamine, NAA, dopamine, 5-HT, taurine, GSH, acetylcysteine, methionine, α-ketoglutarate, succinate and citrate		
	Locomotor measurements on Days 0, 1, 3 and 5 following injections (sensitisation)	No significant correlation with locomotor sensitisation		
	Metabolite deviations showed disruption of TCA cycle, fatty acid metabolism and damage to the mitochondrial electron transport chain in acute and chronic administration between strains	Single dose: ↓ fructose and 5-HT; ↑ lactate, malate, 2-hydroxyglutarate, succinate fumarate, tryptophan and tyrosine	LC–MS and GC–MS	McClay et al., 2013
	Different metabolites contributed to the separation of single exposure group from control than repeated exposure	Chronic administration: ↑ 2-hydroxyglutarate, fructose, sorbitol, putrescine, ergothioneine and Pc		
	Homocarnosine, pantothenate, 4-guanidinobutanoate and *myo*-inositol explained 91% of behavioural sensitisation variation across the eight strains of mice	↑ lactate, malate, 2-hydroxyglutarate, succinate, fumarate, tryptophan and tyrosine; ↓ fructose and 5-HT	LC–MS and GC–MS	Adkins et al., 2013
	Altered energy metabolism, amino acid metabolism and phospholipid metabolism	NAc: ↓ glucose, creatine, glutamate and glutamine, GSH, PE (P-18:0/22:6) and PS (18:0/22:6); ↑ ADP, aspartate and PA (18:0/22:6)	MALDI-MSI	Lin et al., 2019
		Dorsal Hi: ↓ glucose, creatine, glutamate and glutamine, GSH, PE (P-18:0/22:6), PE (16:0/18:1), PE (18:0/22:6) and PS (18:0/22:6); ↑ GMP, ADP and AMP, and aspartate		
		Ventral Hi: ↑ creatine, glutamate, glutamine and aspartate, PA (18:0/22:6) and PEs; ↓ GMP, ADP and AMP		
	Increased dietary trehalose (sugar) partially alleviated the toxic effects of METH	↓ trehalose	GC–MS and MS/MS	Sun, Li, et al., 2011
	Altered carbohydrate metabolism, dysregulation of calcium and iron homeostasis, increased OS and disruption of mitochondrial functions			

TABLE 1 (Continued)

Drug	Main results	Altered metabolites (drug of abuse vs. control)	Analytical method	Reference
	More ion features were significantly altered in hair than in urine	Hair: ↑ acetylcarnitine, 5-methylcytidine, 1-methyladenosine and palmitoyl-L-carnitine; ↓ L-norvaline/betaine/5-aminopentanoate/L-valine, lumichrome, deoxycorticosterone, oleamide, stearamide and hippurate	LC-QTOF-MS	Choi et al., 2017
	Mineralocorticoid, fatty acid amides and mitochondrial fatty acid oxidation	Urine: potential early, late and recent markers of addiction were found but not assigned		
	Altered metabolism of acylcarnitines, amino acids and biogenic amines, glycerophospholipids and sphingolipids	↑ carnitine, decadienylcarnitine and octadecadienylcarnitine; arginine; lysophosphatidylcholine acyl C160, C170, C181 and C204; and sphingomyelin C241, C221 and C241	UPLC-QTOF-ESI-MS (untargeted); AbsoluteIDQ p180 kit (targeted)	Kim et al., 2020
	Altered TCA cycle intermediates, amino acids and other biomolecules	↓ octadecanoylcarnitine and valerylcarnitine; methionine; phosphatidylcholine diacyl C341, C362, C365, C366, C381, C383, C385, C403 and C404; and phosphatidylcholine acyl-alkyl C340, C360, C361, C365, C380, C381, C382, C383, C401, C402, C422 and C423	UHPLC–MS/MS	Lin et al., 2019
		↑ lactate, glutamine, ornithine, niacinamide, histidine, creatinine, ACh, asparagine, glutamate, malic acid, 5-aminolevulinic acid, taurine, 1-methylnicotinamide, citrulline and guanidine acetic acid		
		↓choline, succinate semialdehyde, threonine, glycine, serine, isoleucine, proline, xanthine, creatine, alanine, sulfate, methionine, uric acid, citrate, pyruvic acid, fumarate, *N*-acetyl-L-aspartate, ketoleucine, valine and succinate		

Abbreviations: 5-HIAA, 5-hydroxyindoleacetic acid; Cer, cerebellum; CPP, conditioned-place preference; DOPAC, 3,4-dihydroxyphenylacetic acid; GC-MC, gas chromatography-mass spectrometry; GPC, glycerol phosphocholine; GSH/GSSG, GSH/oxidised GSH; 3-HB, 3-hydroxybutyric acid; Hi, hippocampus; LC, liquid chromatography,NAA, *N*-acetylaspartate; NAc, nucleus accumbens; NAG, *N*-acetyl-glycoprotein; OAG, *O*-acetyl-glycoprotein; Pc, phosphocholine; PFC, prefrontal cortex; Str, striatum; TCA, tricarboxylic acid; Th, thalamus; VTA, ventral tegmental area.

TABLE 2 Brain region-specific changes in metabolite concentrations following chronic morphine treatment versus control animals

Morphine treated vs. control					
		Hi	FCx	NAc	Striatum
Neurotransmitters	Glutamine	↑↓↑*	↓	↑	↑
	Glutamate	↓↑↓*	↓↓↓	↑	↑
	GABA	↑↓↓	↓↑↑	↑	↑
	Succinic acid semialdehyde	↑	↑↑	↑	–
Oxidative stress metabolites	GSH	↓	↓		
	NAA	↑↓*	↑	↑	↑
	Phosphocholine	↓↓	↑		↑
	Myo-inositol	↓↓↑*	↓↓↑*	↓	↓
	Taurine	↓↑↓*	↓	↑	↑
Energy metabolism	Lactic acid	↑↑	↑↑	↑	↑
	Creatine	↓↑	↑↓	↑	↓

Note: Studies conducted in rhesus monkeys and rats (see protocol in Table 1). '↑' indicates increase, '↓' indicates decrease, '□' indicates rhesus monkeys (Deng et al., 2012), '□' indicates rats (Hu et al., 2012), '□' indicates rats (Gao et al., 2007) and '*' indicates disagreement between Hu et al. (2012) and Gao et al. (2007).

Abbreviations: FCx, frontal cortex; Hi, hippocampus; NAA, *N*-acetylaspartate; NAc, nucleus accumbens.

administration, was shown to elicit increased inhibitory and decreased excitatory synapses, whereas the antioxidant compound **platelet-derived growth factor (PDGF)** reverses the synaptic effects of morphine (Cai et al., 2016). Similarly, the antioxidative compound thioredoxin-1 (Trx-1) inhibits morphine-induced conditioned-place preference in transgenic mice by modulating **$GABA_B$** and **dopamine D_1** receptor expression (Li et al., 2018), clearly suggesting a key role for oxidative stress in modulating, at least partly, the reinforcing effects of morphine.

The central (Meng et al., 2012) and peripheral (Zaitsu et al., 2014) biochemical mechanisms underlying the context-dependent learning associated with the rewarding effects of drugs of abuse were investigated in rodents undergoing morphine-induced conditioned-place preference in two independent gas chromatography-mass spectrometry studies. A total of 21 metabolites were observed to significantly differ in the central metabolic profiles of morphine-treated and control mice (Meng et al., 2012). Of these, the elevation of *myo*-inositol and its derivative *myo*-inositol phosphate supports the disrupting action of morphine on membrane integrity and astrocytic morphology and proliferation. The increase in nicotinamide, a product of **nicotinamide adenine dinucleotide** (NAD) metabolism that is also involved in reward memory consolidation, suggests a role of this metabolite in drug-associated learning. The nucleotide **uracil** and the amino acids **proline** and **valine** were also up-regulated. Although indicative of protein breakdown, both proline and valine contribute to Glu and Gln metabolism, further supporting a dysregulation in the Gln–Glu–GABA axis (Meng et al., 2012). The effect of morphine on the plasma and urinary metabolomes was investigated by Zaitsu et al. (2014) in a conditioned-place preference paradigm. Twelve urinary metabolites and four plasma metabolites were strongly predictive of high conditioned-place preference scores (Zaitsu et al., 2014), highlighting the exciting potential for metabolomics to elucidate novel predictive biomarkers for addiction severity. Morphine-conditioned-place preference rats exhibited an increase in *N*-propylamine but a decrease in **3-hydroxybutyric acid** (3-HB), L-tryptophan and cysteine in the plasma compared with control rats and an increase in **2-oxoglutarate**, **fumaric acid**, **malic acid**, **L-threonine** and a decrease in glutamic acid, **isoleucine**, L-valine, **L-aspartic acid**, oxamic acid, 2-aminoethanol, indoxyl sulfate and in the urine. Given that L-tryptophan is elevated in the brain following morphine administration (Messing et al., 1978), a decrease in its circulatory levels suggests that morphine administration results in the uptake of L-tryptophan from the systemic circulation into the brain. Importantly, the increase in TCA intermediates such as 2-oxoglutarate, fumaric acid and malic acid, and the reduction in glutamic acid and 3-hydroxybutyric acid supports the up-regulation of the TCA cycle and the inhibition of β-oxidation of fatty acids and ketone body metabolism for energy production. Similarly, a separate gas chromatography-mass spectrometry-based metabolomic study investigating the metabolic changes in the plasma of rats chronically exposed to an escalating dose of morphine (Liu et al., 2015) reported alterations in TCA cycle intermediates, such as oxalic acid and the malonic acid derivative aminomalonate, alterations in the Gln–Glu–GABA axis, as demonstrated by decreased Gln and increased β-D-glucose, and in membrane components, such as **cholesterol**, **linoleic acid** and **stearic acid**. In line with Zaitsu et al. (2014), a disruption in the metabolism of amino acids and related compounds was also observed by Liu et al. (2015), with decreases in **alanine**, proline, **glycine**, **serine** and threonine. As alanine and glycine are by-products of GABA degradation by the enzyme GABA transaminase, their reduction may be indicative of decreased GABA breakdown. Conversely, proline is associated with both the TCA cycle and the

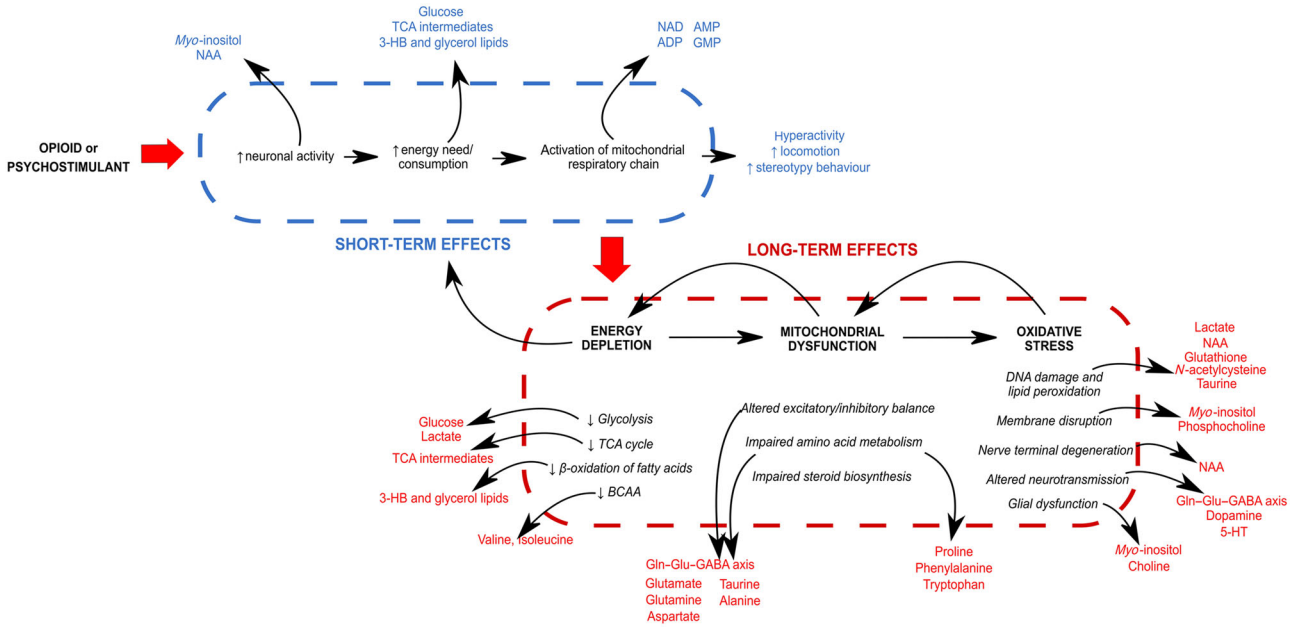

FIGURE 2 Diagram of metabolic alterations caused by drugs of abuse. Metabolites that are altered in response to drug exposure provide information on the underlying cascade of events leading to addiction. As most of the changes leading to an established addiction state are likely to involve adaptive mechanisms, it is important to investigate and discriminate between the short-term effects of acute drug exposure and the long-term, compensatory changes resulting from chronic drug administration (i.e. dependence) on the metabolome. A general mechanism of action of both opioids and psychostimulants seems to involve a short-term increase in energy demand, which leads to long-term energy depletion, mitochondrial dysfunction and oxidative stress. These long-term effects contribute to a cascade of events that feed the cycle of metabolic and pathophysiological derangements characterising addiction, as shown with the backwards arrows. 3-HB, 3-hydroxybutyric acid; Gln, glutamine; Glu, glutamate; NAA, *N*-acetylaspartate; TCA, tricarboxylic acid

pentose phosphate pathway and is involved in **arginine** and Glu metabolism. Once again, these biochemical disruptions point towards dysfunctional energy metabolism.

Several studies have assessed the biochemical effects of common pharmacological interventions used to assist opioid-dependent individuals overcome their dependence. The drug naloxone is an antagonist at the **μ-opioid receptor** used to suppress craving in opioid-dependent individuals undergoing abstinence. The effect of naloxone on the plasma metabolic profile of morphine-treated rats was evaluated by Liu et al. (2015). Rats receiving naloxone after being treated with morphine for 5 days had higher circulating amounts of lactic acid, oxalic acid, aminomalonate, 2-oxoglutarate, β-D-glucose, linoleic acid, cholesterol and **palmitic acid** and reduced alanine, valine, proline, glycine, serine, threonine, **pyroglutamic acid**, hydroxyproline, erythronic acid, Gln, arabinose, rhamnose, isoleucine, **succinate**, 4-hydroxybutanoic acid and **leucine** compared with rats receiving naloxone after saline (Liu et al., 2015). Lower threonine, glycine and serine and higher glucose and oxalic acid were noted in all states (including 'euphoria', 30 min after morphine), implying that disturbances in amino acids (and potentially neurotransmission) and oxidative stress were not recoverable by naloxone and may reflect 'lifetime exposure' to morphine. This demonstrates the potential of metabolomics to elucidate the biochemical processes underlying each stage of the disorder progression.

NMR-based metabolic profiling was used to study various brain regions from morphine-treated rhesus monkeys and rats undergoing detoxification with the long-acting opioid methadone or the α_2 adrenoceptor agonist **clonidine** (Deng et al., 2012; Hu et al., 2012). Upon detoxification, the majority of morphine-induced metabolic variation was normalised to baseline (Deng et al., 2012; Hu et al., 2012), although several metabolites remained altered in specific brain regions (Table 3). Although clonidine was generally more effective than methadone in reversing the biochemical effects of morphine in both species (Deng et al., 2012; Hu et al., 2012), rats showed a more profound reduction in withdrawal symptoms in response to methadone compared with clonidine (Deng et al., 2012). Advanced correlation analysis is warranted to investigate causality between the behavioural effect of pharmacotherapeutic interventions and their effectiveness in restoring predose biochemical profiles.

The effect of 6 days of methadone-aided detoxification on the plasma metabolome was investigated in a human study (Mannelli et al., 2009). An liquid chromatography electrochemical array platform was used to measure purine, monoaminergic and redox metabolites in 14 opioid-dependent individuals undergoing methadone detoxification and 10 nondrug users. Opioid-dependent participants were given methadone orally at 9:00–10:00 AM daily, and blood samples were collected on Days 2 and 3 at 10:00–11:00 AM. The ratio of glutathione (GSH)/oxidised GSH and the antioxidants α-tocopherol and

TABLE 3 Effectiveness of clonidine and methadone detoxification treatment on metabolite deviations caused by morphine treatment

	Withdrawal intervention with clonidine or methadone					
	Rhesus monkey			Rats		
	Hi	FCx	Hi	FCx	NAc	Striatum
Glutamine	✓	–	Clonidine	✓	Clonidine	×
Glutamate	×	×	Methadone	✓	✓	✓
GABA	✓	×	–	Clonidine	Clonidine	×
GSH	×	–	–	✓	–	–
NAA	–	✓	✓	–	✓	✓
Phosphocholine	✓	✓	✓	–	–	✓
Myo-inositol	✓	✓	Clonidine	×	✓	–
Taurine	✓	Methadone	✓	–	Clonidine	✓
Lactic acid	✓	Clonidine	Clonidine	×	Clonidine	Clonidine
Creatine	✓	✓	✓	Clonidine	✓	✓
Succinic acid semialdehyde	–	×	✓	✓	×	–

Note: Studies conducted in rhesus monkeys (Deng et al., 2012) and rats (Hu et al., 2012) (see protocol in Table 1). '✓' indicates both clonidine and methadone treatment restored, '×' indicates neither clonidine nor methadone restored metabolite, 'clonidine' indicates only clonidine restored, 'methadone' indicates only methadone restored and an em dash means there were no results reported.
Abbreviations: FCx, frontal cortex; Hi, hippocampus; NAA, *N*-acetylaspartate; NAc, nucleus accumbens.

γ-tocopherol was significantly higher in opioid-dependent participants, indicating significantly higher oxidative capacity provided for by methadone therapy. Changes in α-tocopherol antioxidant activity are consistent with previous studies evaluating antioxidant serum levels in heroin users undergoing methadone detoxification (Díaz-Flores Estévez et al., 2004; Rodríguez-Delgado et al., 2002). This may indicate a protective effect of methadone in reducing physical opioid withdrawal symptoms by a mechanism involving ROS removal. The increase in plasma **guanine** and xanthosine reported in the methadone group may represent alterations in energy production through the conversion of guanine and xanthosine into their corresponding nucleotides via salvage pathways. The combination of high guanine and low guanosine in the plasma has been shown to be associated with brain toxic insult and increased dopamine turnover (Ciccarelli et al., 1999; Loeffler et al., 1998), whereas guanine-based purines also participate in GABAergic and glutamatergic transmission (Majumder et al., 2007; Schmidt et al., 2007). Significant differences in purine metabolites were found between control and drug-dependent subjects undergoing methadone detoxification (Mannelli et al., 2009), but further investigation is required to assess if any of these metabolites can serve as biological markers of addiction or of response to methadone treatment. No significant differences in **phenylalanine**, tryptophan and **tyrosine** metabolites and monoamines (dopamine, **5-hydroxytryptamine (5-HT; serotonin)** and **noradrenaline**) were found between the groups. However, *N*-methyl-5-HT was present in greater amounts in the plasma of opioid-dependent patients. Interestingly, *N*-methyl-5-HT and its derivative **bufotenine** have also been shown to be elevated in other psychiatric disorders and have been associated with hallucinogenic effects (Takeda et al., 1995), further supporting a common metabolic dysregulation in a range of psychiatric conditions. However, the authors reported that *N*-methyl-5-HT, but none of the other metabolites, was higher in the eight of the 14 drug-dependent participants also tested positive for both **cocaine** and **cannabis** (Mannelli et al., 2009). These results should be viewed as preliminary because of the presence of confounding biological differences between opioid-dependent patients and nondrug users, and in future studies, caution should be taken to control for smoking pattern, age, ethnic background, lifestyle and the diet. Although beyond the scope of this review, the potential of metabolomics to evaluate the interindividual pharmacokinetic properties (thus the ideal, tailored dose) of methadone has been demonstrated and can have implications in the personalised treatment of addiction (Dinis-Oliveira, 2016).

2.2 | Metabolic signature of heroin addiction

Zheng et al. (2013) monitored serum and urinary metabolic changes in response to a 10-day escalating dose of heroin administration in rats, followed by 4 days of abstinence ('withdrawal') and 4 days of readministration of the opioid ('relapse'). Initial heroin administration caused abnormalities in pathways associated with energy metabolism. The concomitant reduction in serum free fatty acids (palmitic acid, linoleic acid, **oleic acid**, nonesterified cholesterol, **docosahexaenoic acid** and octadecanoic acid) and increase in the TCA cycle intermediate citrate in both serum and urine suggest a depletion of fatty acids for energy production and the up-regulation of the TCA cycle as a source of energy. Changes in the concentrations of **aspartate**, hydroxyproline, tryptophan, leucine, valine, phenylalanine, threonine and **thymine** imply that amino acid metabolism

was also perturbed. Elevations in aspartate, the 5-HT metabolite 5-hydroxyindoleacetic acid (5-HIAA) and 5-HT indicate changes in neurotransmission. An effect of heroin administration on membrane integrity is indicated by increased **myo-inositol-1-phosphate** and *myo*-inositol. An increase in circulating *myo*-inositol was detectable early (by Day 5), whereas the increase in aspartate occurred later (between Days 5 and 10), indicating time-dependent changes in the effect of heroin on membrane integrity. These results indicate that membrane disruption precedes (and may be responsible for) changes in amino acid metabolism. After 4 days of abstinence, the urinary and serum metabolomes were comparable with those of controls indicating a rapid return to homeostasis. However, variation was observed in their recovery. Although none of the urinary metabolic abnormalities elicited by drug exposure persisted at withdrawal, serum *myo*-inositol-1-phosphate and threonate remained increased and decreased, respectively. This suggests that membrane damage and long-term abnormalities in synaptic density are a long-term consequence of heroin exposure persisting well into withdrawal (Figure 2). Similar observations to the chronic heroin group were noted in the relapse group, showing deviations from the control group and overlap with the animals that had 10 days of heroin exposure. This indicates that the metabolic state of relapse is comparable with that of long-term heroin exposure (Zheng et al., 2013).

Ning et al. (2018) also compared the serum metabolic profile of rats undergoing heroin self-administration reexposure after a period of abstinence (used to model relapse) to drug-naïve rats. Consistent with previous observations, disruptions were seen in pathways related to energy homeostasis (TCA intermediates and keto bodies), phospholipid cycling (cell membrane components: **choline**, phosphocholine and glycerol phosphocholine) and neurotransmission (amino acids and related molecules: choline, phenylalanine and Gln). However, in contrast to the previous study by Zheng et al. (2013), Ning et al. (2018) observed an inhibition of the TCA cycle, demonstrated by an increase in glucose and decrease in pyruvate and fumarate (and a decrease in lactate). In addition, the ketone bodies 3-hydroxybutyric acid and **acetoacetate** were increased with heroin indicating a shift from oxidative phosphorylation to ketogenesis as an alternative source of energy. These differences may result from the variation in the sampling time points between the studies reflecting the short- and long-term adaptive mechanisms in energy metabolism to heroin administration.

A similar mouse study showed equivalent results in brain samples analysed by ultraperformance liquid chromatography time-of-flight mass spectrometry (Li et al., 2017). Chronic heroin administration disturbed central energy metabolism, demonstrated by an elevation of citrate and nucleotide monophosphates. Increases in the excitatory neurotransmitter Glu, the catecholamines dopamine and **adrenaline**, and the neuromodulators **histamine** and **melatonin** also point towards abnormalities in neurotransmission elicited by chronic heroin use. The elevation of histamine may also link chronic heroin use with the reported activation of mast cells and other components of the immune system in addicted individuals (Galli et al., 1993). A 2-day withdrawal from heroin was sufficient for catecholamines to return to baseline levels, suggestive of an autonomic readjustment during abstinence. In contrast, **histidine** was observed to decrease upon withdrawal, whereas phenylalanine, tryptophan and **N-acetyl-5-HT** increased, pointing to adaptive mechanisms involving the 5-HT system.

These findings are supported by the results of a human study that investigated the hair metabolome of heroin abusers (Xie et al., 2016). The heroin group showed increased concentrations of sorbitol and **cortisol** and decreased concentrations of **arachidonic acid**, GSH, linoleic acid and **myristic acid** (Xie et al., 2016). The impact of heroin on the HPA axis via opioid signalling may underlie the variation noted in cortisol. A decrease in the free fatty acids, arachidonic acid, linoleic acid and myristic acid is consistent with increased energy production, as seen in the mice exposed to heroin (Zheng et al., 2013).

3 | METABOLIC PHENOTYPING OF PSYCHOSTIMULANT ADDICTION

Psychostimulants increase striatal dopamine concentrations by increasing dopamine levels in the nucleus accumbens. Cocaine inhibits the reuptake of dopamine in mesolimbic dopaminergic neurons projecting from the ventral tegmental area to the nucleus accumbens by blocking dopamine transporters located presynaptically, whereas amphetamine and methamphetamine facilitate presynaptic dopamine release. Psychostimulants also stimulate the release of other monoamines such as 5-HT and noradrenaline (Kim et al., 2019). Rodent metabolomic studies using brain tissue have explored the abnormalities in central metabolic processes driven by acute (Kaplan et al., 2013; Li et al., 2012; Olesti et al., 2019) and repeated psychostimulant administration (Adkins et al., 2013; Bu et al., 2013; Kong et al., 2018; Li et al., 2014, 2012; Lin et al., 2019; McClay et al., 2013). Biofluids including urine, blood and hair samples have also been studied to understand the metabolic consequences of exposure (Choi et al., 2017; Goodwin et al., 2014; Olesti et al., 2019; Sánchez-López et al., 2017; Yao et al., 2013), abstinence (Kim et al., 2019; Shima et al., 2011; Zhang, Chiu, et al., 2016; Zheng et al., 2014) and the establishment of drug reinforcement (Zaitsu et al., 2014). Human studies investigating the impact of psychostimulants on hair (Kim et al., 2020) and serum/plasma metabolome (Costa et al., 2019; Lin et al., 2019) and the effect of abstinence from cocaine (Patkar et al., 2009) will also be reviewed. These studies are summarised in Table 1.

3.1 | Metabolic signature of cocaine addiction

The central metabolic signature of rats undergoing both acute and repeated cocaine administration was investigated using NMR spectroscopy-based metabolomics (Li et al., 2012). Seven-day cocaine- conditioned-place preference increased Glu and GABA in the nucleus accumbens and enhanced GAD activity, implying altered neurotransmission along the Gln–Glu–GABA axis. The reported

ability of cocaine to elicit Gln production by glial cells may explain these observations (Sá Santos et al., 2011). These alterations were evident after repeated administration but not after a single dose. Such changes are consistent with what observed with morphine (Gao et al., 2007) indicating a common adaptive, long-term response to chronic drug exposure (Figure 2). Indeed, adaptive functional changes are known to occur at glutamatergic synapses in the nucleus accumbens in response to repeated cocaine administration (Maze et al., 2010). As these changes mirror behavioural sensitisation (Russo et al., 2009; Thomas & Malenka, 2003; Ungless et al., 2001), they represent a key molecular component of the addictive properties of cocaine. Lactate, which is produced via anaerobic metabolism and can be metabolised through the TCA cycle, was decreased after a single dose but increased after chronic administration, indicating a long-term compensatory change in energy metabolism in response to cocaine exposure. An NMR-based study by Kong et al. (2018) suggested that disturbances in energy metabolism may be explained by epigenetic mechanisms. Cocaine-conditioned mice exhibited significantly higher concentrations of nicotinamide mononucleotide and nicotinamide adenine dinucleotide in ventral tegmental area and nucleus accumbens. Nicotinamide mononucleotide and nicotinamide adenine dinucleotide are produced from nicotinamide by the enzyme nicotinamide phosphoribosyltransferase (NAMPT) and play a role in energy metabolism. Nicotinamide phosphoribosyltransferas was shown to be up-regulated in cocaine-conditioned mice via an epigenetic mechanism involving nicotinamide adenine dinucleotide-dependent histone deacetylase **sirtuin 1 (SIRT1)**, thus pointing towards a role for SIRT1 in epigenetic regulation of genes, such as nicotinamide phosphoribosyltransferase, that control energy metabolism (Kong et al., 2018). Altered creatine levels may also be indicative of a shift in normal energy metabolism (Li et al., 2012). The observed dysregulation of creatine (increased in nucleus accumbens and decreased in striatum) and taurine (increased in both areas) has been proposed to reflect oxidative damage. Although an increase in taurine and decrease in its metabolic precursor **cysteine** could indicate the induction of a brain protective mechanism following cocaine administration, a single dose of cocaine induced a reduction in taurine in nucleus accumbens, suggesting a short-term depletion of its antioxidant capacity before the long-term adaptive increase. The concentrations of *N*-acetylaspartate, a marker of neuronal density synthesised in mitochondria, were increased in nucleus accumbens and striatum after both acute and chronic cocaine administration, pointing to an immediate effect of the drug on mitochondrial dysfunction. Finally, membrane damage is indicated by alterations in *myo*-inositol, glycine and choline concentration, which were affected by a single dose of cocaine (Li et al., 2012).

A quantitative evaluation of the global neurobiochemical profile of cocaine-treated rats was achieved by ion mobility mass spectrometry (Kaplan et al., 2013). Acute cocaine administration significantly reduced thalamic and striatal **glucose**, with the greatest decrease seen in the thalami. In the frontal cortex, cocaine exposure increased glucose content, indicating region-specific shifts in glucose metabolism following cocaine treatment. The availability of 5-HT, noradrenaline, glucose, dopamine, 3,4-dihydroxyphenylacetic acid (DOPAC) and 5-HIAA in the thalamus, striatum and prefrontal cortex was also altered as a result of cocaine exposure (Kaplan et al., 2013), indicating abnormalities in neurotransmission induced by the drug. This is consistent with the reported ability of psychostimulants to promote the release of other monoamines such as 5-HT and dopamine (Kim et al., 2019), which is thought to be part of the underlying mechanism of cocaine reward (Sora et al., 2001).

Abnormalities in neurotransmitter metabolism were also reported in brain and blood samples of rats administered with a single dose of cocaine (Olesti et al., 2019) and in the serum of rats undergoing a cocaine self-administration protocol (Goodwin et al., 2014). Using a targeted liquid chromatography–mass spectrometry approach, significant elevations were noted in **acetylcholine (ACh)** in the prefrontal cortex; valine, leucine, GABA, Glu, choline, ACh, **carnitine**, **acetylcarnitine**, creatine, creatinine and **adenosine** in the hippocampus; and choline and adenosine in the striatum. In the cerebellum, Glu, choline, , carnitine and creatinine were increased. In plasma, choline and creatine were increased, whereas creatinine was decreased. Some of these alterations are likely to reflect pharmacological effects of cocaine on the muscle and the brain. For example, cocaine-induced rhabdomyolysis (muscle injury) can lead to altered creatine and creatinine metabolism, with downstream consequences on the brain high-energy phosphate system (Lyoo et al., 2003), whereas the reported inhibition of ChAT by cocaine (Wilson et al., 1994) could explain the increase in hippocampal ACh. A separate study also reported an increase in (3-methoxy-4-hydroxyphenyl)ethylene glycol and **kynurenic acid**, metabolites of noradrenaline and tryptophan, respectively. Both metabolites were previously implicated in cocaine addiction (McDougle et al., 1994; Rockhold et al., 1991) and may be related to disturbances in **catecholamine** (i.e. noradrenaline and dopamine) and 5-HT metabolism. Significant alterations in amino acid metabolism were also reported by an liquid chromatography–mass spectrometry metabolomics study (Sánchez-López et al., 2017), where mice were infused daily for 21 days with cocaine, either alone or administered with **ethanol**. Cocaine alone elevated plasma **methionine** and decreased **argininosuccinic acid** and *N*-ε-acetyl-L-lysine, whereas coinfusion of cocaine and **alcohol** resulted in elevated **carnosine**, **spermidine** and 5-HT and decreased methionine, argininosuccinic acid and *N*-ε-acetyl-L-lysine (Sánchez-López et al., 2017). The derangements in methionine and argininosuccinic acid suggest an overall increase in ROS and **nitric oxide** production, two factors that contribute to liver injury in cocaine-dependent individuals (Aoki et al., 1997). In contrast, *N*-ε-acetyl-L-lysine could provide acetylated **lysine** residues for the epigenetic changes underlying cocaine-based reinforcement.

Biochemical modulations in plasma and urine were assessed in rats undergoing cocaine- conditioned-place preference (Zaitsu et al., 2014). Although significant metabolic changes were found in plasma of cocaine-treated rats (higher L-threonine and *n*-propylamine; lower cysteine and spermidine), no metabolic variation was identified in urine following treatment relative to controls. In a separate rat study by Yao et al. (2013), clear differences were observed in the

urine between cocaine and a control group. Several factors may account for these differences, including differences in animal strain, cocaine dose, length and means of drug administration as well as in chromatographic techniques (liquid chromatography–mass spectrometry n Yao et al., 2013, vs. gas chromatography-mass spectrometry in Zaitsu et al., 2014). Additionally, there is ample evidence that cocaine metabolism differs profoundly between mice and rats, possibly explaining the more marked behavioural and hepatotoxic phenotype in response to cocaine in mice relative to rats (Thompson et al., 1979).

The persistence of biochemical modulations following acute withdrawal from cocaine was studied in the nucleus accumbens of rats 2, 24 and 48 h following a single exposure (Li et al., 2012). The metabolic profiles of the treated animals were distinct from the control group at all time points, indicating that biomolecular alterations persist in the nucleus accumbens up to 48 h after exposure, with only a subset of metabolites returning towards baseline concentrations. A single exposure was not sufficient to cause changes in GABA. However, taurine was significantly decreased and *N*-acetylaspartate was increased as soon as 2 h after a single dose, suggesting that oxidative stress and membrane disruption occur early during the addiction cycle. Interestingly, lactate and phosphocholine remained elevated 48 h after dosing. The involvement of lactate in synaptic plasticity hints at a direct role in consolidating drug-related memories (Hillard, 2005; Wang et al., 2019). Astrocyte-neuron lactate transport in the basolateral amygdala is critical for the reconsolidation of cocaine memory, and strategies reducing lactate concentrations (by blocking glycogenolysis in astrocytes) in the basolateral amygdala of mice undergoing a conditioned-place preference paradigm have been shown to prevent the establishment of cocaine-induced conditioned-place preference and to decrease cocaine self-administration (Zhang, Xue, et al., 2016). Importantly, although GABA was not dysregulated after a single cocaine exposure nor after repeated administration, it was significantly altered in mice exposed to cocaine- conditioned-place preference, highlighting that contextual conditioning of a drug is able to induce metabolite changes in the brain, which are independent of the effect of the drug administration per se. Therefore, the inclusion of a group of animals treated with the drug but not undergoing conditioned-place preference should be considered when investigating cocaine- conditioned-place preference effects on the metabolome. In a separate study, the metabolic perturbations in energy supply (creatine, creatinine and adenosine), oxidative stress (GSH and spermidine), neurotransmission (pyroglutamic acid, Gln, Glu and GABA), mitochondrial function (carnosine) and membrane integrity (choline) induced by cocaine self-administration were still evident after 1-day abstinence in prefrontal cortex, striatum and nucleus accumbens but normalised at Week 3 in all brain areas except the striatum (Zhang, Chiu, et al., 2016). The finding that cocaine use leads to long-term metabolic abnormalities in the striatum may explain the presence of drug craving long after withdrawal from the drug (Volkow et al., 2006).

Understanding the metabolic changes occurring upon drug withdrawal is important to shine light on the biochemical mechanisms underlying recovery from addiction. A human study involving 18 cocaine-dependent individuals investigated the effect of 2 weeks of abstinence on their plasma metabolic profile (Patkar et al., 2009). This study found significant alterations in purine and tryptophan metabolism, as reported in opioid-dependent individuals upon detoxification (Mannelli et al., 2009), but no changes in oxidative stress-related metabolites. It is generally believed that oxidative stress might be applicable for acute rather than more prolonged intoxication, which may explain these findings. Plasma metabolic profiles from cocaine-dependent individuals were correlated with their addiction severity index (ASI) drug scores. Specifically, *N*-methyl-5-HT accounted for 62% of variance in severity of drug abuse based on addiction severity index drug score,and combined with xanthine it accounted for 73%. These findings implicate plasma *N*-methyl-5-HT and **xanthine** as good candidate biomarkers for assessing and predicting addiction severity. In accordance with Mannelli et al. (2009), no significant changes in 5-HT metabolism were observed, indicating that the biosynthesis of 5-HT from tryptophan was unaffected by cocaine. Instead, the increase in *N*-methyl-5-HT suggests a dysregulation of the enzyme that metabolises 5-HT to *N*-methyl-5-HT following chronic cocaine exposure. This hypothesis requires further investigation and future studies with larger sample sizes and more appropriate controls are warranted.

3.2 | Metabolic signature of methamphetamine addiction

The animal studies investigating the metabolic effects of methamphetamines have reported contradicting findings. Similar to what was observed for cocaine, several studies reported disrupted energy metabolism as a consequence of chronic methamphetamines intake (Kim et al., 2019; Shima et al., 2011; Zheng et al., 2014). A significant depletion of TCA cycle intermediates (Shima et al., 2011; Zheng et al., 2014) and branched-chain amino acids (Kim et al., 2019; Zheng - et al., 2014) was observed in the blood and urine of rats repeatedly exposed to methamphetamines. On the other hand, no change in TCA intermediates was detected in plasma and urine after methamphetamine- conditioned-place preference training (Zaitsu et al., 2014). As glycolysis is down-regulated upon drug deprivation (Muneer et al., 2011), it can be speculated that the metabolic effect of methamphetamine on the TCA cycle is due to acute withdrawal and cannot be elicited by a chronic conditioned-place preference paradigm. Collectively, these results suggest that different drug administration protocols have distinct effects on plasma and urine metabolic signatures, possibly as a result of adaptive mechanisms to repeated drug use and/or to the presence or absence of contextual learning (i.e. conditioned-place preference). A common finding to these studies was altered lipid metabolism. Reduced plasma **lauric acid** and increased urinary stearic acid were induced by methamphetamine-conditioned-place preference (Zaitsu et al., 2014). In the absence of contextual learning, methamphetamine elicited changes in the β-oxidation of free fatty acids and the formation of 3-hydroxybutyric acid, indicative of altered lipid turnover, as well as changes in

glycerophospholipids and sphingolipids, suggestive of membrane breakdown, in both urine and blood, although the direction of change is unclear (Shima et al., 2011; Zheng et al., 2014). Changes to lipid metabolism may represent a compensatory mechanism to meet the increased energy demand induced by methamphetamine exposure. Methamphetamine was seen to elicit different effects on some lipids compared with heroin. For example, serum *myo*-inositol and *myo*-inositol-1-phosphate was increased in response to heroin (Zheng et al., 2013) but reduced in response to methamphetamine (Zheng et al., 2014). Further evidence of altered energy metabolism in response to methamphetamine comes from a study performed on *Drosophila melanogaster* (Sun, Li, et al., 2011). Flies fed on a methamphetamine-supplemented diet had lower circulating trehalose, the major blood sugar in the *Drosophila*, indicating higher metabolic rates and/or increased glycolysis. Interestingly, trehalose supplementation increased the flies' lifespan, indicating that methamphetamine toxicity is linked to a depletion of energy cofactors and that replenishing these cofactors may attenuate the negative effects of the drug (Sun, Li, et al., 2011).

The change in the concentrations of neuroactive compounds in the blood of methamphetamine-treated animals additionally suggests altered excitability at the CNS level following methamphetamine intake. Zheng et al. (2014) observed increased aspartate and Glu but lower alanine and glycine in the serum of rats chronically exposed to methamphetamine. Kim et al. (2019) reported a reduction in plasma phenylalanine, tyrosine and tryptophan biosynthesis pathways with methamphetamines, indicative of a potential downstream effect on catecholaminergic and monoaminergic neurotransmission. In support of this hypothesis, increases in tryptophan and tyrosine and decreases in 5-HT were reported in the whole brain of mice treated with a single methamphetamine dose (McClay et al., 2013). This study investigated the different mechanisms underlying acute and chronic methamphetamine exposure. Although acute methamphetamine treatment elicited alterations in energy related metabolites (e.g. reduced fructose, increased lactate, malate, 2-hydroxyglutarate, succinate and fumarate), chronic methamphetamine-administered mice had higher amounts of the sugars fructose and sorbitol, the antioxidants **putrescine** and ergothioneine, and the membrane component phosphocholine compared with the control animals (Adkins et al., 2013; McClay et al., 2013). These results suggest that acute administration is characterised by disrupted energy metabolism and alterations in neurotransmitters and fatty acid metabolism, whereas the chronic effects of methamphetamine are further associated with oxidative stress and membrane damage.

Bu et al. (2013) and Lin et al. (2019) also demonstrated impaired energy metabolism, along with changes in neurotransmitter and oxidative stress metabolites in the brain of chronically methamphetamine-treated rats. These metabolites were predominantly related to GABA, monoamine and oxidative stress metabolites, as well as TCA cycle intermediates and indicators of neuronal membrane disruption. Bu et al. (2013) reported decreases in dopamine, Gln and Glu in the hippocampus, nucleus accumbens and prefrontal cortex, consistent with previous models of chronic methamphetamine administration (Moszczynska et al., 2004; Thomas et al., 2008). The decrease of Gln and Glu mirrored the decrease of GABA and 2-oxoglutarate, which is partly due to decreased TCA cycle activity and, possibly, increased Glu uptake. Succinic acid semialdehyde levels increased, consistent with its role as an intermediate of GABA catabolism. A decrease in Glu and Gln was also observed in the nucleus accumbens and dorsal hippocampus by Lin et al. (2019), although these metabolites, along with the amino acid and excitatory neurotransmitter aspartate, were down-regulated in the ventral hippocampus. Together, these findings suggest that the disturbance to Gln–Glu–GABA axis in the brain may be involved in the behavioural sensitisation to methamphetamine. Together with a general increase in nucleotides like **ADP**, **GMP** and **AMP** in nucleus accumbens and dorsal hippocampus (but a decrease in the ventral hippocampus), these findings point towards an alteration in energy homeostasis in a brain region-dependent manner. A reduction in the antioxidant GSH was reported in both studies (Bu et al., 2013; Lin et al., 2019). Moreover, a reduction in *N*-acetylaspartate and an increase of phosphocholine were observed in brain regions of chronically treated rats, indicating that oxidative damage was present alongside neuronal and mitochondrial dysfunction (Bu et al., 2013). The increase in **homocysteine**, an amino acid and precursor of methionine, could be regarded as an indicator of apoptosis and neuronal hypersensitivity to excitation as well as DNA damage (Kruman et al., 2000). Moreover, the increase in homocysteine may be caused by the inhibition of methionine synthesis by methamphetamine (Chandra et al., 2006), leading to changes in DNA methylation. Increased *myo*-inositol and phosphocholine are consistent with membrane disruption (Bu et al., 2013) and may reflect cell death due to the severely neurotoxic properties of methamphetamine (Zheng et al., 2014). Phospholipids were generally down-regulated in nucleus accumbens and dorsal hippocampus but up-regulated in the ventral hippocampus (Lin et al., 2019), suggesting region-specific effects of methamphetamine treatment. Finally, Bu et al. (2013) found no significant correlation between metabolic disruptions and locomotor sensitisation behaviour. Given that locomotor sensitisation is linked to increased craving and vulnerability to relapse (Robinson & Berridge, 1993; Vanderschuren & Pierce, 2020), this finding suggests that these metabolites may have poor predictive potential. Future studies are needed to determine whether a conditioned-place preference design and the resulting contextual learning are needed in order to find a significant correlation with locomotor sensitisation.

Mass spectrometric analysis of the metabolic effects of repeated methamphetamine self-administration in rat urine and hair revealed abnormalities in the metabolism of mineralocorticoid, fatty acid amides and mitochondrial fatty acid oxidation (Choi et al., 2017). In the urine, ion features corresponding to potential urine markers of methamphetamine addiction were detected but only putatively assigned. In the hair, a decrease in **deoxycorticosterone** suggests altered central production of neurosteroids (Mellon & Griffin, 2002), whereas an increase in carnitine and acylcarnitines is indicative of elevated metabolic capacity by mitochondrial oxidation of fatty acids. The reduction observed in the fatty acid amides **oleamide** and

stearamide, known to interact with endocannabinoid, glutamatergic and GABAergic signalling, may indicate a modulation of central neurotransmission. The authors concluded that methamphetamine evoked more dramatic metabolic changes in the hair than in the urine. This may reflect the greater stability of hair and longer accrual of biochemical information related to drug-induced metabolic perturbations compared with urine samples. As such, hair metabolomics should be considered as a non-invasive way to profile the addiction status of an individual.

A study conducted on the hair metabolome of methamphetamine users revealed additional abnormalities in the abundance of amino acids and lipids (Kim et al., 2020). The amino acids arginine and methionine, both known ROS scavengers (Liang et al., 2018; Luo & Levine, 2009), were down-regulated in the hair of drug abusers, which may indicate higher susceptibility to oxidative stress. Lower phosphatidylcholines, but higher **lysophosphatidylcholines** and sphingomyelin, suggested a dramatic dysregulation of lipid biosynthesis/metabolism pathways, which is consistent with what was reported from animal models of methamphetamine exposure (Kim et al., 2019; Lin et al., 2019) as well as human studies on cocaine and methamphetamine abusers (Ross et al., 2002). These observations point to the possibility that chronic drug use activates **phospholipase A2**, the enzyme that cleaves phosphatidylcholine into lysophosphatidylcholine. The elevation of acylcarnitines is consistent with findings from animal studies (Kim et al., 2019) and suggests abnormal β-oxidation of fatty acids and mitochondrial dysfunction. A reduction in carnitines (both free and acetylated forms) and lower long-chain fatty acids was also reported in the fasting serum metabolic profile of crack-cocaine users (Costa et al., 2019). The circulating levels of lactate, histidine and tyrosine were also elevated in the crack group. Thus, increased energy needs induced by crack abuse may result in disrupt the mitochondria (indicated by carnitine/fatty acid metabolism), resulting in a shift to alternative energy sources (elevation of lactate) and the altered biosynthesis of neurotransmitters (histamine and catecholamines from histidine and tyrosine respectively) (Figure 2). In the serum, metabolites that were dysregulated in methamphetamine-addicted individuals included TCA intermediates, amino acids and other biomolecules (Lin et al., 2019). An increase in excitatory amino acids (Gln, **asparagine** and Glu) and a decrease in inhibitory amino acids (glycine and alanine) point to an increase in brain activity induced by the drug. ACh was also elevated (whereas choline was reduced) in the plasma of methamphetamine users, collected at fasting (Lin et al., 2019). Similar findings associated with altered energy metabolism, steroid biosynthesis, amino acid and fatty acid metabolism were reported in response to other types of psychostimulants, such as **MDMA**, amphetamine and mephedrone in human plasma (Nielsen et al., 2016; Steuer et al., 2020), suggesting a common mechanism of action.

Despite the lack of human studies investigating the metabolic consequences of abstinence from methamphetamines, three of the rodent studies presented above examined the effects of withdrawal on the metabolic phenotype. Shima et al. (2011) reported that the methamphetamine-induced plasma and urinary alterations (mainly associated with altered TCA intermediates, amino acids and fatty acids) persisted 24 h after the last drug administration but were not evident at 96 h. In a separate study, 2 days of detoxification was generally sufficient to restore the serum and urinary metabolic profile of methamphetamine-treated rats to pretreatment levels (Zheng et al., 2014). In the serum, several amino acids including Gln, Glu and aspartate (involved in neurotransmission and energy metabolism) were completely restored, whereas fatty acids like arachidonic acid, decanedioic acid, stearic acid and glycerol-3-phosphate (involved in membrane stability and energy metabolism) were only partially recovered. Isoleucine, palmitic acid, creatinine, citrate and 2-oxoglutarate did not return to pretreatment values. In urine, only lactate was persistently altered after withdrawal (Zheng et al., 2014). Similarly, Kim et al. (2019) reported that 12- or 24-h abstinence resulted in the reversal of the metabolic abnormalities in glycerophospholipids, sphingolipids and most amino acids elicited by methamphetamine self-administration. However, the concentrations of aspartate, Glu and glycine remained significantly lower than controls 12 and 24 h after the last methamphetamine administration. Acetylcarnitines and biogenic amines were further altered during abstinence, suggesting that the dynamic response of the metabolome to methamphetamine exposure spans at least 24 h following the last administration. Moreover, 5-HT exhibited a short-term increase (immediately after self-administration) but a long-term decrease after methamphetamine exposure (12 and 24 h after the last exposure). Similarly, pathway analysis demonstrated a decrease in the phenylalanine, tyrosine and tryptophan biosynthesis and in the valine, leucine and isoleucine biosynthesis pathways immediately after self-administration but an increase after 12 and 24 h relative to controls. These results highlight the importance of investigating the time profile of metabolic responses to drugs of abuse, which may provide biomarkers relevant for discriminating addiction states. Moreover, the time when the metabolic change occurs may inform on whether the change is the result of a short-term molecular mechanism or of a longer term compensatory mechanism (e.g. transcriptional/epigenetics). Exploring these molecular mechanisms may help to guide the development of interventional strategies for clinical practice.

4 | FUTURE PERSPECTIVES

In recent years, findings from metabolomic studies have provided a metabolic perspective to the addiction cycle that complements our neurophysiological and neuropharmacological knowledge (Figure 2). These studies have shown that opioid and psychostimulant addiction results in largely overlapping metabolic derangements. The increase in energy demand observed in such studies as a short-term consequence of drug exposure reflects the pharmacological profile of those drugs on the brain and other organs. As the individual transitions towards a state of dependence, metabolomic studies reveal biochemical changes indicative of mitochondrial dysfunction (e.g. *N*-acetylaspartate), cell death and oxidative stress (e.g. lactate,

choline and taurine), and energy depletion. Such alterations are reflective of known adaptations induced by long-term administration of drugs of abuse on the brain and other organs. Energy depletion, for instance, may be reflective of the presence of a homeostatic compensatory mechanism, which opposes the chronic pharmacological effect of the drug. In relation to the brain, this includes (i) the broadly characterised suppression of the mesolimbic reward pathway (decline of basal dopamine levels and **D_2 receptor** levels in the striatum), which is thought to underline some of the emotional withdrawal symptoms and craving induction commonly experienced in dependence, and (ii) the hypofunctioning of the frontal cortex, which is associated with impaired decision making and loss of top-down control over drug administration, rendering the behaviour 'automatic'. Impairment of interrelated cellular processes of mitochondria metabolism, oxidative stress and apoptosis assessed by membrane potential and respiratory chain activity, by elevation of indictors of oxidative stress (e.g. SOD and GSH) and by TUNEL staining has consistently been reported in the brain, heart and liver, following long-term administration of substances of abuse, although diversity exists in relation to the severity of those effects. Nonetheless, these changes have been associated with addictive behaviour pathology, neurotoxicity, cardio-toxicity and cognitive decline among other pathological consequences of long-term drug abuse. Alterations in neurotransmitters and their precursors balance (e.g. dopamine, 5-HT and Gln–Glu–GABA axis) following chronic drug use identified from metabolomic studies are consistent with neurochemical adaptations reported in the brain via other experimental approaches. These are reflective of compensatory homeostatic neuroadaptations, which underline the behavioural manifestations of addiction (e.g. tolerance, physical and emotional withdrawal symptoms and relapse).

With the emergence of metabolomics, biomarker research has shifted from the hypothesis-driven study of single molecules to the simultaneous measurement of thousands of compounds with no a priori knowledge. This hypothesis-generating approach facilitates the identification of biochemical pathways involved in pathological processes and the discovery of new pharmacological targets. Understanding the biochemical changes occurring at each stage of the addiction cycle can facilitate the identification of diagnostic and prognostic biomarker panels to provide objective measures of addiction and rehabilitation. Despite the success of metabolomics in clinical research, its translation to clinical practice has been undermined by issues of reproducibility and cost. Clinical metabolomics relies on the comparison of the metabolic profile of a single individual with 'healthy' reference ranges. Thus, the existence of standardised protocols of sample collection, preparation, data analysis and metabolite identification, along with the selection of an appropriate control population and validated quality control pipelines, needs to be in place before metabolomics can be routinely applied in the clinic. Targeted analysis of a small panel of diagnostic/prognostic markers measured in easily accessible samples, such as urine, blood or hair, could be routinely run to objectively monitor an individual's progress. By leveraging individual differences in the metabolome, metabolomics provides an objective measure that can inform personalised approaches to addiction to maximise the chances of recovery. Well-characterised longitudinal studies where the metabolic profile of an individual is measured at baseline, before the initiation of pharmacological detoxification therapies, will allow to identify early predictive markers and personalised treatment strategies tailored to the metabolome of the individual patient. The prediction of addiction outcomes based on neuroimaging data has already been successful (Reske & Paulus, 2008). The use of metabolic markers quantified from non-invasive samples (e.g. urine and hair) could offer a more feasible and cost-effective method to bring precision medicine to clinical practice.

5 | CONCLUSION

In recent years, the misuse of prescription opioids in the United States has led to what is currently known as the 'opioid epidemic', a public health crisis costing $26 billion to the US healthcare system and 16,000 deaths in 2013 alone (Florence et al., 2016). Identifying markers of addiction can help identify those at risk and lower the rate of fatalities. Drug abuse affects 35 million people worldwide (United Nations, 2020), and with a relapse rate of 40–60% (National Institute on Drug Abuse [NIDA], 2020), achieving personalised and effective treatment options is a pressing issue. Metabolomic techniques performed on accessible samples offer great promise to facilitate the implementation of precision medicine interventions to achieve faster diagnosis and better treatment efficacy based upon an individual's metabolic phenotype.

5.1 | Nomenclature of targets and ligands

Key protein targets and ligands in this article are hyperlinked to corresponding entries in the IUPHAR/BPS Guide to PHARMACOLOGY http://www.guidetopharmacology.org, and are permanently archived in the Concise Guide to PHARMACOLOGY 2019/20 (Alexander et al., 2019).

ACKNOWLEDGEMENT

G.C. is supported by the Medical Research Council (MRC) (Grant MR/N014103/1).

AUTHOR CONTRIBUTIONS

G.C. and V.S. planned and drafted the manuscript. N.S. verified and cross-referenced the information presented in the review with the original primary papers. J.R.S. and A.B. provided support throughout the writing process by sharing their expertise in the field of metabolomics and addiction, respectively. All authors contributed to the final manuscript.

CONFLICT OF INTEREST

The authors declare no conflicts of interest.

DATA AVAILABILITY STATEMENT

Data sharing is not applicable to this article because no new data were created or analysed in this study.

ORCID

Giorgia Caspani https://orcid.org/0000-0003-1697-1437
Jonathan R. Swann https://orcid.org/0000-0002-6485-4529
Alexis Bailey https://orcid.org/0000-0003-1541-1964

REFERENCES

Adkins, D. E., Mcclay, J. L., Vunck, S. A., Batman, A. M., Vann, R. E., Clark, S. L., Souza, R. P., Crowley, J. J., Sullivan, P. F., van den Oord, E. J. C. G., & Beardsley, P. M. (2013). Behavioral metabolomics analysis identifies novel neurochemical signatures in methamphetamine sensitization. *Genes, Brain and Behavior*, *12*, 780–791. https://doi.org/10.1111/gbb.12081

Alexander, S. P. H., Christopoulos, A., Davenport, A. P., Kelly, E., Mathie, A., Peters, J. A., Veale, E. L., Armstrong, J. F., Faccenda, E., Harding, S. D., Pawson, A. J., Sharman, J. L., Southan, C., Davies, J. A., & CGTP Collaborators. (2019). The Concise Guide to PHARMACOLOGY 2019/20: G protein-coupled receptors. *British Journal of Pharmacology*, *176*, S21–S141.

American Psychiatric Association. (2000). *American Psychiatric Association: Diagnostic and statistical manual of mental disorders* (Fourth ed.). Text Revision

Aoki, K., Ohmori, M., Takimoto, M., Ota, H., & Yoshida, T. (1997). Cocaine-induced liver injury in mice is mediated by nitric oxide and reactive oxygen species. *European Journal of Pharmacology*, *336*, 43–49. https://doi.org/10.1016/S0014-2999(97)01230-2

Bu, Q., Lv, L., Yan, G., Deng, P., Wang, Y., Zhou, J., Yang, Y., Li, Y., & Cen, X. (2013). NMR-based metabonomic in hippocampus, nucleus accumbens and prefrontal cortex of methamphetamine-sensitized rats. *Neurotoxicology*, *36*, 17–23. https://doi.org/10.1016/j.neuro.2013.02.007

Cai, Y., Yang, L., Hu, G., Chen, X., Niu, F., Yuan, L., Liu, H., Xiong, H., Arikkath, J., & Buch, S. (2016). Regulation of morphine-induced synaptic alterations: Role of oxidative stress, ER stress, and autophagy. *The Journal of Cell Biology*, *215*, 245–258. https://doi.org/10.1083/jcb.201605065

Chandra, G., Gangopadhyay, P. K., Senthil Kumar, K. S., & Mohanakumar, K. P. (2006). Acute intranigral homocysteine administration produces stereotypic behavioral changes and striatal dopamine depletion in Sprague–Dawley rats. *Brain Research*, *1075*, 81–92. https://doi.org/10.1016/j.brainres.2005.12.073

Choi, B., Kim, S. P., Hwang, S., Hwang, J., Yang, C. H., & Lee, S. (2017). Metabolic characterization in urine and hair from a rat model of methamphetamine self-administration using LC-QTOF-MS-based metabolomics. *Metabolomics*, *13*, 1–17.

Ciccarelli, R., Di Iorio, P., Giuliani, P., D'Alimonte, I., Ballerini, P., Caciagli, F., & Rathbone, M. P. (1999). Rat cultured astrocytes release guanine-based purines in basal conditions and after hypoxia/hypoglycemia. *Glia*, *25*, 93–98. https://doi.org/10.1002/(SICI)1098-1136(19990101)25:1<93::AID-GLIA9>3.0.CO;2-N

Costa, T. B. B. C., Lacerda, A. L. T., Mas, C. D., Brietzke, E., Pontes, J. G. M., Marins, L. A. N., Martins, L. G., Nunes, M. V., Pedrini, M., Carvalho, M. S. C., Mitrovitch, M. P., Hayashi, M. A. F., Saldanha, N. L., Poppi, R. J., & Tasic, L. (2019). Insights into the effects of crack abuse on the human metabolome using a NMR approach. *Journal of Proteome Research*, *18*, 341–348. https://doi.org/10.1021/acs.jproteome.8b00646

Deng, Y., Bu, Q., Hu, Z., Deng, P., Yan, G., Duan, J., Hu, C., Zhou, J., Shao, X., Zhao, J., Li, Y., Zhu, R., Zhao, Y., & Cen, X. (2012). ^{1}H-nuclear magnetic resonance-based metabonomic analysis of brain in rhesus monkeys with morphine treatment and withdrawal intervention. *Journal of Neuroscience Research*, *90*, 2154–2162. https://doi.org/10.1002/jnr.23109

Díaz-Flores Estévez, J. F., Díaz-Flores Estévez, F., Hernández Calzadilla, C., Rodríguez Rodríguez, E. M., Díaz Romero, C., & Serra-Majem, L. (2004). Application of linear discriminant analysis to the biochemical and haematological differentiation of opiate addicts from healthy subjects: A case–control study. *European Journal of Clinical Nutrition*, *58*, s449–s455.

Dinis-Oliveira, R. J. (2016). Metabolomics of methadone: Clinical and forensic toxicological implications and variability of dose response. *Drug Metabolism Reviews*, *48*, 568–576. https://doi.org/10.1080/03602532.2016.1192642

Dole, V. P., & Nyswander, M. E. (1967). Heroin addiction—A metabolic disease. *Archives of Internal Medicine*, *120*, 19–24. https://doi.org/10.1001/archinte.1967.00300010021004

Feng, Y. M., Jia, Y. F., Su, L. Y., Wang, D., Lv, L., Xu, L., & Yao, Y. G. (2013). Decreased mitochondrial DNA copy number in the hippocampus and peripheral blood during opiate addiction is mediated by autophagy and can be salvaged by melatonin. *Autophagy*, *9*, 1395–1406. https://doi.org/10.4161/auto.25468

Florence, C. S., Zhou, C., Luo, F., & Xu, L. (2016). The economic burden of prescription opioid overdose, abuse, and dependence in the United States, 2013. *Medical Care*, *54*, 901–906. https://doi.org/10.1097/MLR.0000000000000625

Galli, S. J., Tsai, M., & Wershil, B. K. (1993). The c-kit receptor, stem cell factor, and mast cells. What each is teaching us about the others. *The American Journal of Pathology*, *142*, 965–974.

Gao, H., Xiang, Y., Sun, N., Zhu, H., Wang, Y., Liu, M., Ma, Y., & Lei, H. (2007). Metabolic changes in rat prefrontal cortex and hippocampus induced by chronic morphine treatment studied *ex vivo* by high resolution ^{1}H NMR spectroscopy. *Neurochemistry International*, *50*, 386–394. https://doi.org/10.1016/j.neuint.2006.09.012

Goodwin, C. R., Sherrod, S. D., Marasco, C. C., Bachmann, B. O., Schramm-Sapyta, N., Wikswo, J. P., & McLean, J. A. (2014). Phenotypic mapping of metabolic profiles using self-organizing maps of high-dimensional mass spectrometry data. *Analytical Chemistry*, *86*, 6563–6571. https://doi.org/10.1021/ac5010794

Gustavsson, A., Svensson, M., Jacobi, F., Allgulander, C., Alonso, J., Beghi, E., Dodel, R., Ekman, M., Faravelli, C., Fratiglioni, L., Gannon, B., Jones, D. H., Jennum, P., Jordanova, A., Jönsson, L., Karampampa, K., Knapp, M., Kobelt, G., Kurth, T., … CDBE2010 Study Group. (2011). Cost of disorders of the brain in Europe 2010. *European Neuropsychopharmacology*, *21*, 718–779. https://doi.org/10.1016/j.euroneuro.2011.08.008

Hillard, C. J. (2005). Lipids and drugs of abuse. *Life Sciences*, *77*, 1531–1542. https://doi.org/10.1016/j.lfs.2005.05.004

Hu, Z., Deng, Y., Hu, C., Deng, P., Bu, Q., Yan, G., Zhou, J., Shao, X., Zhao, J., Li, Y., Zhu, R., Xu, Y., Zhao, Y., & Cen, X. (2012). ^{1}H NMR-based metabonomic analysis of brain in rats of morphine dependence and withdrawal intervention. *Behavioural Brain Research*, *231*, 11–19. https://doi.org/10.1016/j.bbr.2012.02.026

Kaddurah-Daouk, R., & Weinshilboum, R. M. (2014). Pharmacometabolomics: Implications for clinical pharmacology and systems pharmacology. *Clinical Pharmacology and Therapeutics*, *95*, 154–167. https://doi.org/10.1038/clpt.2013.217

Kang, L., Dai, Z. Z., Li, H. H., & Ma, L. (2006). Environmental cues associated with morphine modulate release of glutamate and γ-aminobutyric acid in ventral subiculum. *Neuroscience Bulletin*, *22*, 255–260.

Kaplan, K. A., Chiu, V. M., Lukus, P. A., Zhang, X., Siems, W. F., Schenk, J. O., & Hill, H. H. Jr. (2013). Neuronal metabolomics by ion mobility mass spectrometry: Cocaine effects on glucose and selected biogenic amine metabolites in the frontal cortex, striatum, and

thalamus of the rat. *Analytical and Bioanalytical Chemistry*, *405*, 1959–1968. https://doi.org/10.1007/s00216-012-6638-7

Kim, S., Jang, W. J., Yu, H., Kim, J., Lee, S. K., Jeong, C. H., & Lee, S. (2020). Revealing metabolic perturbation following heavy methamphetamine abuse by human hair metabolomics and network analysis. *International Journal of Molecular Sciences*, *21*, 6041. https://doi.org/10.3390/ijms21176041

Kim, S., Jang, W. J., Yu, H., Ryu, I. S., Jeong, C. H., & Lee, S. (2019). Integrated non-targeted and targeted metabolomics uncovers dynamic metabolic effects during short-term abstinence in methamphetamine self-administering rats. *Journal of Proteome Research*, *18*, 3913–3925. https://doi.org/10.1021/acs.jproteome.9b00363

Kong, J., Du, C., Jiang, L., Jiang, W., Deng, P., Shao, X., Zhanga, B., Lia, Y., Zhua, R., Zhaoa, Q., Fua, D., Gua, H., Luoa, L., Longa, H., Zhaoa, Y., & Cena, X. (2018). Nicotinamide phosphoribosyltransferase regulates cocaine reward through Sirtuin 1. *Experimental Neurology*, *307*, 52–61. https://doi.org/10.1016/j.expneurol.2018.05.010

Koob, G., & Kreek, M. J. (2007). Stress, dysregulation of drug reward pathways, and the transition to drug dependence. *The American Journal of Psychiatry*, *164*, 1149–1159. https://doi.org/10.1176/appi.ajp.2007.05030503

Koob, G. F., & Le Moal, M. (2001). Drug addiction, dysregulation of reward, and allostasis. *Neuropsychopharmacology*, *24*, 97–129. https://doi.org/10.1016/S0893-133X(00)00195-0

Kosmides, A. K., Kamisoglu, K., Calvano, S. E., Corbett, S. A., & Androulakis, I. P. (2013). Metabolomic fingerprinting: Challenges and opportunities. *Critical Reviews in Biomedical Engineering*, *41*, 205–221. https://doi.org/10.1615/CritRevBiomedEng.2013007736

Kruman, I. I., Culmsee, C., Chan, S. L., Kruman, Y., Guo, Z., Penix, L. R., & Mattson, M. P. (2000). Homocysteine elicits a DNA damage response in neurons that promotes apoptosis and hypersensitivity to excitotoxicity. *The Journal of Neuroscience*, *20*, 6920–6926. https://doi.org/10.1523/JNEUROSCI.20-18-06920.2000

Li, H., Bu, Q., Chen, B., Shao, X., Hu, Z., Deng, P., Lv, L., Deng, Y., Zhu, R., Li, Y., Zhang, B., Hou, J., du, C., Zhao, Q., Fu, D., Zhao, Y., & Cen, X. (2014). Mechanisms of metabonomic for a gateway drug: Nicotine priming enhances behavioral response to cocaine with modification in energy metabolism and neurotransmitter level. *PLoS ONE*, *9*, e87040. https://doi.org/10.1371/journal.pone.0087040

Li, R. S., Takeda, T., Ohshima, T., Yamada, H., & Ishii, Y. (2017). Metabolomic profiling of brain tissues of mice chronically exposed to heroin. *Drug Metabolism and Pharmacokinetics*, *32*, 108–111. https://doi.org/10.1016/j.dmpk.2016.10.410

Li, X., Huang, M., Yang, L., Guo, N., Yang, X., Zhang, Z., Bai, M., Ge, L., Zhou, X., Li, Y., & Bai, J. (2018). Overexpression of thioredoxin-1 blocks morphine-induced conditioned place preference through regulating the interaction of γ-aminobutyric acid and dopamine systems. *Frontiers in Neurology*, *9*, 309. https://doi.org/10.3389/fneur.2018.00309

Li, Y., Yan, G. Y., Zhou, J. Q., Bu, Q., Deng, P. C., Yang, Y. Z., Lv, L., Deng, Y., Zhao, J. X., Shao, X., Zhu, R. M., Huang, Y. N., Zhao, Y. L., & Cen, X. B. (2012). ^{1}H NMR-based metabonomics in brain nucleus accumbens and striatum following repeated cocaine treatment in rats. *Neuroscience*, *218*, 196–205. https://doi.org/10.1016/j.neuroscience.2012.05.019

Liang, M., Wang, Z., Li, H., Cai, L., Pan, J., He, H., Wu, Q., Tang, Y., Ma, J., & Yang, L. (2018). L-Arginine induces antioxidant response to prevent oxidative stress via stimulation of glutathione synthesis and activation of Nrf2 pathway. *Food and Chemical Toxicology*, *115*, 315–328. https://doi.org/10.1016/j.fct.2018.03.029

Lin, M., Xu, J., Liu, X., Dai, Z., Liu, Z., Zhao, X., Sun, Y., & Pu, X. (2019). Metabolomics profiling of methamphetamine addicted human serum and three rat brain areas. *RSC Advances*, *9*, 41107–41119. https://doi.org/10.1039/C9RA08096A

Liu, R., Cheng, J., Yang, J., Ding, X., Yang, S., Dong, F., Guo, N., & Liu, S. (2015). GC-MS-based plasma metabolomic investigations of morphine dependent rats at different states of euphoria, tolerance and naloxone-precipitated withdrawal. *Metabolic Brain Disease*, *30*, 767–776. https://doi.org/10.1007/s11011-014-9638-9

Loeffler, D. A., Lewitt, P. A., Juneau, P. L., Camp, D. M., Demaggio, A. J., Milbury, P., Matson, W. R., & Rathbone, M. P. (1998). Altered guanosine and guanine concentrations in rabbit striatum following increased dopamine turnover. *Brain Research Bulletin*, *45*, 297–299. https://doi.org/10.1016/S0361-9230(97)00367-5

Luo, S., & Levine, R. L. (2009). Methionine in proteins defends against oxidative stress. *The FASEB Journal*, *23*, 464–472. https://doi.org/10.1096/fj.08-118414

Lyoo, I. K., Kong, S. W., Sung, S. M., Hirashima, F., Parow, A., Hennen, J., Cohen, B. M., & Renshaw, P. F. (2003). Multinuclear magnetic resonance spectroscopy of high-energy phosphate metabolites in human brain following oral supplementation of creatine-monohydrate. *Psychiatry Research: Neuroimaging*, *123*, 87–100. https://doi.org/10.1016/S0925-4927(03)00046-5

Majumder, P., Trujillo, C. A., Lopes, C. G., Resende, R. R., Gomes, K. N., Yuahasi, K. K., Britto, L. R. G., & Ulrich, H. (2007). New insights into purinergic receptor signaling in neuronal differentiation, neuroprotection, and brain disorders. *Purinergic Signal*, *3*, 317–331. https://doi.org/10.1007/s11302-007-9074-y

Mannelli, P., Patkar, A., Rozen, S., Matson, W., Krishnan, R., & Kaddurah-Daouk, R. (2009). Opioid use affects antioxidant activity and purine metabolism: Preliminary results. *Human Psychopharmacology*, *24*, 666–675. https://doi.org/10.1002/hup.1068

Maze, I., Covingtoni, H. E., Dietz, D. M., Laplant, Q., Renthal, W., Russo, S. J., Mechanic, M., Mouzon, E., Neve, R. L., Haggarty, S. J., Ren, Y., Sampath, S. C., Hurd, Y. L., Greengard, P., Tarakhovsky, A., Schaefer, A., & Nestler, E. J. (2010). Essential role of the histone methyltransferase G9a in cocaine-induced plasticity. *Science*, *327*, 213–216.

McClay, J. L., Adkins, D. E., Vunck, S. A., Batman, A. M., Vann, R. E., Clark, S. L., Beardsley, P. M., & van den Oord, E. J. C. G. (2013). Large-scale neurochemical metabolomics analysis identifies multiple compounds associated with methamphetamine exposure. *Metabolomics*, *9*, 392–402. https://doi.org/10.1007/s11306-012-0456-y

McDougle, C. J., Black, J. E., Malison, R. T., Zimmermann, R. C., Kosten, T. R., Heninger, G. R., & Price, L. H. (1994). Noradrenergic dysregulation during discontinuation of cocaine use in addicts. *Archives of General Psychiatry*, *51*, 713–719. https://doi.org/10.1001/archpsyc.1994.03950090045007

Mellon, S. H., & Griffin, L. D. (2002). Neurosteroids: Biochemistry and clinical significance. *Trends in Endocrinology and Metabolism*, *13*, 35–43. https://doi.org/10.1016/S1043-2760(01)00503-3

Meng, J., Zhang, X., Wu, H., Bu, J., Shi, C., Deng, C., & Mao, Y. (2012). Morphine-induced conditioned place preference in mice: Metabolomic profiling of brain tissue to find 'molecular switch' of drug abuse by gas chromatography/mass spectrometry. *Analytica Chimica Acta*, *710*, 125–130. https://doi.org/10.1016/j.aca.2011.09.033

Messing, R. B., Flinchbaugh, C., & Waymire, J. C. (1978). Changes in brain tryptophan and tyrosine following acute and chronic morphine administration. *Neuropharmacology*, *17*, 391–396. https://doi.org/10.1016/0028-3908(78)90011-4

Miguel-Hidalgo, J. J. (2009). The role of glial cells in drug abuse. *Current Drug Abuse Reviews*, *2*, 76–82. https://doi.org/10.2174/1874473710902010076

Moszczynska, A., Fitzmaurice, P., Ang, L., Kalasinsky, K. S., Schmunk, G. A., Peretti, F. J., Aiken, S. S., Wickham, D. J., & Kish, S. J. (2004). Why is parkinsonism not a feature of human methamphetamine users? *Brain*, *127*, 363–370. https://doi.org/10.1093/brain/awh046

Muneer, P. M. A., Alikunju, S., Szlachetka, A. M., & Haorah, J. (2011). Methamphetamine inhibits the glucose uptake by human neurons and astrocytes: Stabilization by acetyl-L-carnitine. *PLoS ONE*, *6*, e19258. https://doi.org/10.1371/journal.pone.0019258

National Institute on Drug Abuse. (2020). How effective is drug addiction treatment?

Nielsen, K. L., Telving, R., Andreasen, M. F., Hasselstrøm, J. B., & Johannsen, M. (2016). A metabolomics study of retrospective forensic data from whole blood samples of humans exposed to 3,4-methylenedioxymethamphetamine: A new approach for identifying drug metabolites and changes in metabolism related to drug consumption. *Journal of Proteome Research*, *15*, 619–627. https://doi.org/10.1021/acs.jproteome.5b01023

Ning, T., Leng, C., Chen, L., Ma, B., & Gong, X. (2018). Metabolomics analysis of serum in a rat heroin self-administration model undergoing reinforcement based on ^{1}H-nuclear magnetic resonance spectra. *BMC Neuroscience*, *19*, 1–9.

Olesti, E., Rodríguez-Morató, J., Gomez-Gomez, A., Ramaekers, J. G., de la Torre, R., & Pozo, O. J. (2019). Quantification of endogenous neurotransmitters and related compounds by liquid chromatography coupled to tandem mass spectrometry. *Talanta*, *192*, 93–102. https://doi.org/10.1016/j.talanta.2018.09.034

Patkar, A. A., Rozen, S., Mannelli, P., Matson, W., Pae, C. U., Krishnan, K. R., & Kaddurah-Daouk, R. (2009). Alterations in tryptophan and purine metabolism in cocaine addiction: A metabolomic study. *Psychopharmacology*, *206*, 479–489. https://doi.org/10.1007/s00213-009-1625-1

Ramshini, E., Alaei, H., Reisi, P., Naghdi, N., Afrozi, H., Alaei, S., Alehashem, M., & Eftekharvaghefi, S. (2019). Effect of intracerebroventricular injection of GABA receptors antagonists on morphine-induced changes in GABA and GLU transmission within the mPFC: An in vivo microdialysis study. *Iranian Journal of Basic Medical Sciences*, *22*, 246–250. https://doi.org/10.22038/ijbms.2019.28478.6925

Reske, M., & Paulus, M. P. (2008). Predicting treatment outcome in stimulant dependence. *Annals of the new York Academy of Sciences*, *1141*, 270–283. https://doi.org/10.1196/annals.1441.011

Robinson, T. E., & Berridge, K. C. (1993). The neural basis of drug craving: An incentive-sensitization theory of addiction. *Brain Research Reviews*, *18*(3), 247–291. https://doi.org/10.1016/0165-0173(93)90013-p

Rockhold, R. W., Oden, G., Ho, I. K., Andrew, M., & Farley, J. M. (1991). Glutamate receptor antagonists block cocaine-induced convulsions and death. *Brain Research Bulletin*, *27*, 721–723. https://doi.org/10.1016/0361-9230(91)90052-L

Rodríguez-Delgado, M. A., Díaz-Flores Estévez, J. F., Díaz-Flores Estévez, F., Hernández Calzadilla, C., & Díaz Romero, C. (2002). Fast determination of retinol and α-tocopherol in plasma by LC. *Journal of Pharmaceutical and Biomedical Analysis*, *28*, 991–997. https://doi.org/10.1016/S0731-7085(02)00051-1

Ross, B. M., Moszczynska, A., Peretti, F. J., Adams, V., Schmunk, G. A., Kalasinsky, K. S., Ang, L., Mamalias, N., Turenne, S. D., & Kish, S. J. (2002). Decreased activity of brain phospholipid metabolic enzymes in human users of cocaine and methamphetamine. *Drug and Alcohol Dependence*, *67*, 73–79. https://doi.org/10.1016/S0376-8716(02)00022-4

Russo, S. J., Wilkinson, M. B., Mazei-Robison, M. S., Dietz, D. M., Maze, I., Krishnan, V., Renthal, W., Graham, A., Birnbaum, S. G., Green, T. A., Robison, B., Lesselyong, A., Perrotti, L. I., Bolanos, C. A., Kumar, A., Clark, M. S., Neumaier, J. F., Neve, R. L., Bhakar, A. L., … Nestler, E. J. (2009). Nuclear factor κB signaling regulates neuronal morphology and cocaine reward. *The Journal of Neuroscience*, *29*, 3529–3537. https://doi.org/10.1523/JNEUROSCI.6173-08.2009

Sá Santos, S., Sonnewald, U., Carrondo, M. J. T., & Alves, P. M. (2011). The role of glia in neuronal recovery following anoxia: In vitro evidence of neuronal adaptation. *Neurochemistry International*, *58*, 665–675. https://doi.org/10.1016/j.neuint.2011.02.005

Saccenti, E., Hoefsloot, H. C. J., Smilde, A. K., Westerhuis, J. A., & Hendriks, M. M. W. B. (2014). Reflections on univariate and multivariate analysis of metabolomics data. *Metabolomics*, *10*, 361–374. https://doi.org/10.1007/s11306-013-0598-6

Sánchez-López, E., Marcos, A., Ambrosio, E., Mayboroda, O. A., Marina, M. L., & Crego, A. L. (2017). Investigation on the combined effect of cocaine and ethanol administration through a liquid chromatography–mass spectrometry metabolomics approach. *Journal of Pharmaceutical and Biomedical Analysis*, *140*, 313–321. https://doi.org/10.1016/j.jpba.2017.03.061

Schmidt, A. P., Lara, D. R., & Souza, D. O. (2007). Proposal of a guanine-based purinergic system in the mammalian central nervous system. *Pharmacology & Therapeutics*, *116*, 401–416. https://doi.org/10.1016/j.pharmthera.2007.07.004

Sepúlveda, J., Oliva, P., & Contreras, E. (2004). Neurochemical changes of the extracellular concentrations of glutamate and aspartate in the nucleus accumbens of rats after chronic administration of morphine. *European Journal of Pharmacology*, *483*, 249–258. https://doi.org/10.1016/j.ejphar.2003.10.037

Shima, N., Miyawaki, I., Bando, K., Horie, H., Zaitsu, K., Katagi, M., Bamba, T., Tsuchihashi, H., & Fukusaki, E. (2011). Influences of methamphetamine-induced acute intoxication on urinary and plasma metabolic profiles in the rat. *Toxicology*, *287*, 29–37. https://doi.org/10.1016/j.tox.2011.05.012

Sora, I., Hall, F. S., Andrews, A. M., Itokawa, M., Li, X. F., Wei, H. B., Wichems, C., Lesch, K. P., Murphy, D. L., & Uhl, G. R. (2001). Molecular mechanisms of cocaine reward: Combined dopamine and serotonin transporter knockouts eliminate cocaine place preference. *Proceedings of the National Academy of Sciences of the United States of America*, *98*, 5300–5305. https://doi.org/10.1073/pnas.091039298

Spanagel, R., & Weiss, F. (1999). The dopamine hypothesis of reward: Past and current status. *Trends in Neurosciences*, *22*, 521–527. https://doi.org/10.1016/S0166-2236(99)01447-2

Steuer, A. E., Kaelin, D., Boxler, M. I., Eisenbeiss, L., Holze, F., Vizeli, P., Czerwinska, J., Dargan, P. I., Abbate, V., Liechti, M. E., & Kraemer, T. (2020). Comparative untargeted metabolomics analysis of the psychostimulants 3,4-methylenedioxy-methamphetamine (MDMA), amphetamine, and the novel psychoactive substance mephedrone after controlled drug administration to humans. *Metabolites*, *10*(8), 306. https://doi.org/10.3390/metabo10080306

Stiene-Martin, A., Gurwell, J. A., & Hauser, K. F. (1991). Morphine alters astrocyte growth in primary cultures of mouse glial cells: Evidence for a direct effect of opiates on neural maturation. *Brain Research. Developmental Brain Research*, *60*, 1–7. https://doi.org/10.1016/0165-3806(91)90149-D

Sun, J. Y., Yang, J. Y., Wang, F., Wang, J. Y., Song, W., Su, G. Y., Dong, Y. X., & Wu, C. F. (2011). Lesions of nucleus accumbens affect morphine-induced release of ascorbic acid and GABA but not of glutamate in rats. *Addiction Biology*, *16*, 540–550. https://doi.org/10.1111/j.1369-1600.2010.00244.x

Sun, L., Li, H. M., Seufferheld, M. J., Walters, K. R., Margam, V. M., Jannasch, A., Diaz, N., Riley, C. P., Sun, W., Li, Y. F., Muir, W. M., Xie, J., Wu, J., Zhang, F., Chen, J. Y., Barker, E. L., Adamec, J., & Pittendrigh, B. R. (2011). Systems-scale analysis reveals pathways involved in cellular response to methamphetamine. *PLoS ONE*, *6*, e18215. https://doi.org/10.1371/journal.pone.0018215

Takeda, N., Ikeda, R., Ohba, K., & Kondo, M. (1995). Bufotenine reconsidered as a diagnostic indicator of psychiatric disorders. *Neuroreport*, *6*, 2378–2380. https://doi.org/10.1097/00001756-199511270-00024

Thomas, D. M., Francescutti-Verbeem, D. M., & Kuhn, D. M. (2008). The newly synthesized pool of dopamine determines the severity

of methamphetamine-induced neurotoxicity. *Journal of Neurochemistry*, *105*, 605–616. https://doi.org/10.1111/j.1471-4159.2007.05155.x

Thomas, M. J., & Malenka, R. C. (2003). Synaptic plasticity in the mesolimbic dopamine system. *Philosophical Transactions of the Royal Society of London. Series B: Biological Sciences*, *358*, 815–819. https://doi.org/10.1098/rstb.2002.1236

Thompson, M. L., Shuster, L., & Shaw, K. (1979). Cocaine-induced hepatic necrosis in mice—The role of cocaine metabolism. *Biochemical Pharmacology*, *28*, 2389–2395. https://doi.org/10.1016/0006-2952(79)90705-6

Tsuji, M., Nakagawa, Y., Ishibashi, Y., Yoshii, T., Takashima, T., Shimada, M., & Suzuki, T. (1996). Activation of ventral tegmental $GABA_B$ receptors inhibits morphine-induced place preference in rats. *European Journal of Pharmacology*, *313*, 169–173. https://doi.org/10.1016/0014-2999(96)00642-5

Ungless, M. A., Whistler, J. L., Malenka, R. C., & Bonci, A. (2001). Single cocaine exposure in vivo induces long-term potentiation in dopamine neurons. *Nature*, *411*, 583–587. https://doi.org/10.1038/35079077

United Nations. (2020). World drug report 2020.

Vanderschuren, L. J. M. J., & Pierce, R. C. (2020). Sensitization processes in drug addiction. In D. Self & J. Staley Gottschalk (Eds.), *Behavioral Neuroscience of Drug Addiction. Current Topics in Behavioral Neurosciences* (Vol. 3). Berlin, Heidelberg: Springer. https://doi.org/10.1007/7854_2009_21

Veech, R. L. (1991). The metabolism of lactate. *NMR in Biomedicine*, *4*, 53–58. https://doi.org/10.1002/nbm.1940040204

Volkow, N. D., Wang, G. J., Telang, F., Fowler, J. S., Logan, J., Childress, A. R., Jayne, M., Ma, Y., & Wong, C. (2006). Cocaine cues and dopamine in dorsal striatum: Mechanism of craving in cocaine addiction. *The Journal of Neuroscience*, *26*, 6583–6588. https://doi.org/10.1523/JNEUROSCI.1544-06.2006

Wang, Q., Hu, Y., Wan, J., Dong, B., & Sun, J. (2019). Lactate: A novel signaling molecule in synaptic plasticity and drug addiction. *BioEssays*, *41*, 1900008. https://doi.org/10.1002/bies.201900008

Wee, S., & Koob, G. F. (2010). The role of the dynorphin–κ opioid system in the reinforcing effects of drugs of abuse. *Psychopharmacology*, *210*, 121–135. https://doi.org/10.1007/s00213-010-1825-8

Westerink, B. H. C., Kwint, H. F., & DeVries, J. B. (1996). The pharmacology of mesolimbic dopamine neurons: A dual-probe microdialysis study in the ventral tegmental area and nucleus accumbens of the rat brain. *The Journal of Neuroscience*, *16*, 2605–2611. https://doi.org/10.1523/JNEUROSCI.16-08-02605.1996

Wilson, J. M., Carroll, M. E., Lac, S. T., DiStefano, L. M., & Kish, S. J. (1994). Choline acetyltransferase activity is reduced in rat nucleus accumbens after unlimited access to self-administration of cocaine. *Neuroscience Letters*, *180*, 29–32. https://doi.org/10.1016/0304-3940(94)90906-7

Worley, B., & Powers, R. (2013). Multivariate analysis in metabolomics. *Current Metabolomics*, *1*, 92–107. https://doi.org/10.2174/2213235X11301010092

Xie, P., Wang, T. J., Yin, G., Yan, Y., Xiao, L. H., Li, Q., & Bi, K. S. (2016). Metabonomic study of biochemical changes in human hair of heroin abusers by liquid chromatography coupled with ion trap-time of flight mass spectrometry. *Journal of Molecular Neuroscience*, *58*, 93–101. https://doi.org/10.1007/s12031-015-0655-x

Yao, D., Shi, X., Wang, L., Gosnell, B. A., & Chen, C. (2013). Characterization of differential cocaine metabolism in mouse and rat through metabolomics-guided metabolite profiling. *Drug Metabolism and Disposition*, *41*, 79–88. https://doi.org/10.1124/dmd.112.048678

Zaitsu, K., Miyawaki, I., Bando, K., Horie, H., Shima, N., Katagi, M., Tatsuno, M., Bamba, T., Sato, T., Ishii, A., Tsuchihashi, H., Suzuki, K., & Fukusaki, E. (2014). Metabolic profiling of urine and blood plasma in rat models of drug addiction on the basis of morphine, methamphetamine, and cocaine-induced conditioned place preference. *Analytical and Bioanalytical Chemistry*, *406*, 1339–1354. https://doi.org/10.1007/s00216-013-7234-1

Zhang, X., Chiu, V. M., Todd, R. P., Sorg, B. A., & Hill, H. H. (2016). Neuronal metabolomics by ion mobility mass spectrometry in cocaine self-administering rats after early and late withdrawal. *Analytical and Bioanalytical Chemistry*, *408*, 4233–4245. https://doi.org/10.1007/s00216-016-9508-x

Zhang, Y., Xue, Y., Meng, S., Luo, Y., Liang, J., Li, J., Ai, S., Sun, C., Shen, H., Zhu, W., Wu, P., Lu, L., & Shi, J. (2016). Inhibition of lactate transport erases drug memory and prevents drug relapse. *Biological Psychiatry*, *79*, 928–939. https://doi.org/10.1016/j.biopsych.2015.07.007

Zheng, T., Liu, L., Aa, J., Wang, G., Cao, B., Li, M., Shi, J., Wang, X., Zhao, C., Gu, R., Zhou, J., Xiao, W., Yu, X., Sun, R., Zhou, Y., Zuo, Y., & Zhu, X. (2013). Metabolic phenotype of rats exposed to heroin and potential markers of heroin abuse. *Drug and Alcohol Dependence*, *127*, 177–186. https://doi.org/10.1016/j.drugalcdep.2012.06.031

Zheng, T., Liu, L., Shi, J., Yu, X., Xiao, W., Sun, R., Zhou, Y., Aa, J., & Wang, G. (2014). The metabolic impact of methamphetamine on the systemic metabolism of rats and potential markers of methamphetamine abuse. *Molecular BioSystems*, *10*, 1968–1977. https://doi.org/10.1039/C4MB00158C

How to cite this article: Caspani G, Sebők V, Sultana N, Swann JR, Bailey A. Metabolic phenotyping of opioid and psychostimulant addiction: A novel approach for biomarker discovery and biochemical understanding of the disorder. *Br J Pharmacol*. 2021;1–29. https://doi.org/10.1111/bph.15475